Advances in Nano Research, *Vol. 17, No. 6 (2024) 575-591*
https://doi.org/10.12989/anr.2024.17.6.575

Shear deformable-based kinematic model for static analysis of G-Ori composite panel

Ali Basem[1], Mohanad Hatem Shadhar[2], Yasser M. Kadhim[3], Ranganathaswamy M.K.[4], Raman Kumar[5,6], Barno Abdullaeva[7], Ibrahim Mahariq[*8,9,10], Essam Althaqafi[11] and Saiful Islam[11]

[1]*Faculty of Engineering, Warith Al-Anbiyaa University, Karbala 56001, Iraq*
[2]*Department of Civil Engineering, College of Engineering, Al-Iraqia University, Baghdad, Iraq*
[3]*Civil Engineering Department, College of Engineering, Al-Nahrain University, Iraq*
[4]*Department of Mechanical Engineering, School of Engineering and Technology, JAIN (Deemed to be University), Bangalore, Karnataka, India*
[5]*School of Mechanical Engineering, Rayat Bahra University, Kharar, Punjab 140103, India*
[6]*Faculty of Engineering, Sohar University, PO Box 44, Sohar, PCI 311, Oman*
[7]*Department of Mathematics and Information Technologies, Vice-Rector for Scientific Affairs, Tashkent State Pedagogical University, Tashkent, Uzbekistan*
[8]*GUST Engineering and Applied Innovation Research Center (GEAR), Gulf University for Science and Technology, Mishref, Kuwait*
[9]*Applied Science Research Center, Applied Science Private University, Amman, Jordan*
[10]*Department of Medical Research, China Medical University Hospital, China Medical University, Taichung, Taiwan*
[11]*Civil Engineering Department, College of Engineering, King Khalid University, Abha 61421, Saudi Arabia*

(*Received October 3, 2024, Revised November 28, 2024, Accepted December 9, 2024*)

Abstract. In this work, an analytical-based formulation for static bending analysis of a G-Ori reinforced shell in cylindrical form subjected to thermomechanical loads is presented. The governing equations are derived using a shear deformable-based kinematic model. The virtual work principle is used to derived governing equations in terms of in-plane displacement and rotations components. The solution procedure is extended in an analytical manner using the Navier's technique. To constitute the behavioral relations, the effective material properties of graphene origami nanofiller in a copper matrix are derived using the statistical and experimental relations. The effective material properties are evaluated using the Halpin-Tsai micromechanical model and rule of mixture. The parametric results are obtained in terms of thermal loads, volume fraction and folding parameter. Some numerical results in tabular form is presented to investigated impact of content and folding characteristics of G-Ori on the static bending results. The results show a decrease in transverse deflection with an addition in graphene origami content. It is deduced that the transverse deflection is decreased about 20% with a 2% enhancement in the graphene origami content.
Keywords: cylindrical panel; folding characteristics; graphene origami; shear deformable model; virtual work principle

1. Introduction

Introduction of novel materials for application in advanced structures and systems is new challenge for material scientists and engineers. The new structures with foldable micro structures are introduced for application in controllable structures. These materials and structures can be used in various situations with controllability properties due to its changeable properties in thermal environments and hydrogenation process. The foldable nanostructure reinforced composites are recently used in engineering structures. The main problem in analysis and design of foldable structures is estimation of the effective thermal and mechanical material properties of the graphene origami reinforced structures using the statistical and experimental methods. The literature review is organized here to show importance of graphene nanoplatelets, graphene sheets and recently introduced graphene origami.

*Corresponding author, Ph.D.,
E-mail: ibmahariq@gmail.com

Punera and Kant (2021) employed a novel corrected shear deformable model for dynamic/static bending responses of sandwich laminated panel using the analytical methods. The governing equations were derived using the Hamilton's principle and the modified Bai *et al*. (2020) studied temperature dependent behaviors of metal un-saturated soils using solution of the coupled nonlinear contaminant-heat-moisture equations. The effect of various parameters of moisture environment and thermal ambient was studied on the coupled nonlinear responses. Ye *et al*. (2023) extended an Isogeometric-based formulation for free vibration/static results of a cylindrical sandwich panel rested on an elastic foundation through 2D discrete method and curvilinear kinematic relations. They show efficiency and importance of suggested method for handling the solution procedure in curved boundaries. Singh and Kumari (2020) studied effect of various distribution of different layers on the vibration responses of hybrid sandwich composite panel with various boundary conditions through Hamiltonian formulation. The weak formulation was extended to derive distribution of electric potential, displacement, strain and stress components. The solution procedure was developed through employing the extended Kantorovich method for conversion of the

ISSN: 2287-237X (Print), 2287-2388 (Online)

partial differential equations. Bai *et al*. (2017) studied the effect of velocity of the fluids on the penetration characteristics of a porous material and its impact on the absorption capacity of mentioned material. The general solution for particle's migration was developed for a porous media.

Jam *et al*. (2013) studied the impact of various edge conditions on the static distribution of stress and deformation in a hybrid sandwich panel using a novel numerical method named as generalized differential quadrature method. Deformability of the sandwich panel was modeled using the lower order shear deformation theory. The impact of grid points was studied on the numerical trends of the results. Lopatin and Morozov (2021) studied effect of complete clamped edge conditions on the dynamic formulation of sandwich panel made of elastic materials using the Galerkin's approach. The required mode shapes for vibrational behavior were obtained from the static bending analysis. Authors verified their formulation and numerical results using the finite element based numerical packages. Bai *et al*. (2023) studied the effect of temperature on the mechanical properties of geo-polymers enriched with the alkali activator in the extended range of ambient temperature. Charles *et al*. (1972) studied effect of curved girder on the elastic bending of cylindrical panels using the Rayleigh-Ritz method. The results were extended in terms of geometric parameters. Banoqitah *et al*. (2022) studied natural frequency analysis of carbon nanotube reinforced structure. Khadimallah *et al*. (2024) extended nonlocal theory for stability response analysis of microtubules. Mercan *et al*. (2018) employed singular convolution method for vibration analysis of reinforced plate. Abouelregal *et al*. (2021) investigated impact of cylindrical hole on the behavior of unbounded structure. Solbhani *et al*. (2022) studied a parametric analysis on the vibration analysis of various shell structures composed of graphene nanoplatelets.

Babaei and Eslami (2021) extended a new perturbation-based solution procedure for numerical solution of the large deflection behavior of cylindrical panel subjected to mechanical and thermal loads through a shear deformable model. The bending results of small scale panel was studied using the nonlocal strain gradient theory with accounting neutral surface effect. Rahbar Ranji and Rostami Hoseynabadi (2012) included effect of various loading type and edge conditions on the static bending responses of circular cylindrical panel using the semi analytical methods. For example, Guo *et al*. (2019) reported details of two experimental works regarding preparation of SiO2 nano-composites with graphene sheets using the hydrothermal reaction. Du *et al*. (2021) extended a single step operation for application of carbon fibers as reinforcement in a folded structure using graphene origami. Some analytical approaches were developed for providing upper and lower limits of out of plane and in plane compressive strengths. Various characteristics such as failure modes, history of deformation and compressive strengths of manufactures composite structure were computed using theoretical, numerical and experimental analyses. Yang *et al*. (2023) suggested application of folded structures in a doubly curved structures for application in bending analysis. The shell was subjected to mechanical loads and the constituent materials were simulated as a nanocomposite structure with effective material properties in which the Halpin-Tsai micro-mechanical model was used in order to constitute material properties. An enhancement in bending deflection is observed with an increase in foldability characteristics and a decrease in content of graphene content.

Vali and Arefi (2023) employed a higher-order kinematic based formulation for vibrational characteristic analysis of graphene origami porous cylindrical panel in thermal and mechanical environment. Hamilton's principle and generalized three dimensional Hooke's law were extended in three dimensional state in order to derived governing equations of motion. After applying an analytical method, the results indicated that maximum natural frequencies are obtained for X-type pattern of folded reinforcement. Importance of these materials in reflecting an extended response and providing a wide range of dynamic responses with major tuneability in terms of temperature and foldability was explained in detail. Furthermore, an overview on the effect of wave number and various patterns of nanofillers was presented. Fan and Shen (2022) defined characteristics and importance of graphene origami as a metamaterial with solid phase in micro scales. It was confirmed that the overall material properties of graphene origami inside a copper matric reflects a general anisotropic property and a negative Poisson's ratio. Furthermore, temperature dependent material properties of those materials was explained in detail. Zhao *et al*. (2021) presented an atomistic overview on the new metamaterials with negative Poisson's ratio using a programmable manufacturing process. In order to overcome the serious conditions of some auxetic materials due to local exceed deformations or high loading failures, the graphene origami was metamaterials was introduced with excellent tuneability. A more range of negative values for Poisson's ration and higher values for elasticity modulus was reported through this experimental work. Nguyen and Phan (2023) studied nonlinear vibration analysis of a porous plate made of bi directionally functionally graded materials through a nonlinear kinematic model using an isogeometric analysis.

Ranjbar and Feli (2019) studied effect of temperature dependent material properties on the low velocity impact analysis of a micro beam reinforced with novel nanofillers. Ray (2023) presented an elasticity formulation for analysis of doubly curved shells composed of antisymmetric composite layers. Tornabene (2016) employed a higher-order kinematic formulation for vibration analysis of doubly curved shells in various shapes. Arefi and Mohammad-Rezaei Bidgoli (2019) studied effect of an initial electric potential on the stress and displacement analysis of the smart doubly curved shells. Effect of thermal loads as well as lateral pressure was studied on the stability responses of rectangular nanoplates by Shen *et al*. (2021). As instance, Wang *et al*. (2023a) organized a novel work on the production of nano-reinforced composites. Using the recycled fibers in the production of nanocomposite structures yields to a material bonded through hydrogen bonding. Qu *et al*. (2021) used first order plate theory for thickness stretching analysis of a piezoelectric semi-conductor plate. Thai and Choi (2014) developed a three-

part transverse field for closed form solution of a plate made of functionally graded materials. Meng *et al*. (2021) extended a novel process for conversion of two dimensional graphene sheets structure to three dimensional structures through a folding process where a chemical process including hydrogenation was used. Continuum-based formulation as well as molecular dynamic simulation were extended in order to evaluate Miura-ori effective properties. Programmability and tuneability of the constituent materials were explained with changes of important parameters.

Characteristics of graphene origami based composite metamaterial through a hydrogenation process was illustrated by Guo *et al*. (2023). They concluded on the effect of various dispersion of folded microstructures and thermal loads on the overall material properties of composite structure. Effect of characteristics of folded structure was examined on the wave dispersion characteristics and general behavior of enabled structure. Murari *et al*. (2019) used a Timoshenko framework for investigating the vibrational behavior of enabled metamaterial nanocomposite beam reinforced with folded nanomaterials where the reinforcements were dispersed with a layerwise pattern along the thickness direction. Differential quadrature numerical method was extended for investigating the impact of foldability characteristics as well as content and dispersion patterns of folded graphene on the dynamic responses. Some experimental works were suggested for preparation and characterization of graphene based nanocomposite structures. There are some important works on the modeling and material science of graphene and origami materials in the literature.

Bai *et al*. (2022, 2023b, 2024a, b, c) provided the detailed procedures for providing the novel material compositions. The novel method for analysis of joint distribution was addressed by Bao *et al*. (2025). One can find some new analysis on the nano material analysis and effective material properties by Cui *et al*. (2024), Chen *et al*. (2024), Fu *et al*. (2023) and Fan *et al*. (2024a, b). The new material with energy consumption property and electroelastic property for application in battery was illustrated by Gao *et al*. (2023) and Guo *et al*. (2024). Huang *et al*. (2024 a, b) and Han *et al*. (2022 a, b, 2025) illustrated application of novel materials and new methods for application in advanced investigations. The novel properties of metamaterials such as acoustic and energy consumption properties of the advanced composite materials were illustrated by Ji *et al*. (2023), Kong *et al*. (2024), Lai *et al*. (2024), Liang *et al*. (2024a) and Long *et al*. (2024). Multi-functional applications of the materials and structures subjected to multi-load condition were illustrated by Li *et al*. (2024a, b, 2025), Lv *et al*. (2024) and Lu (2024). Metamaterial-based materials and compositions using the 4D-Printing and data analysis of composed structure were developed by Pi *et al*. (2025), Peng *et al*. (2024a), Ren *et al*. (2024), Shi *et al*. (2024) and Song *et al*. (2024). There is electrical properties of novel materials for application in various situations as reported by Wang *et al*. (2023b, 2024 a, b, c) and Wu *et al*. (2024). There are some studies about application of nanomaterials and metamaterial structures with innovative applications as reported by Xiao *et al*. (2022), Xu *et al*. (2023), Yan *et al*. (2024) and Yu *et al*. (2021, 2025). The new nanocomposite materials are used for application in the dynamic loading and consequently an impact analysis is required for this type of material. There are some theoretical works on the crack analysis in various materials by Zhang *et al*. (2014, 2015, 2018, 2020, 2023a).

The literature review with studying the more related works on the novel material and strictures and various production methods was presented in the Introduction section. Furthermore, we provided a deep review on the nanostructures such as graphene sheets, graphene platelets and graphene origami. The effective material properties of aforementioned nanofillers reinforced structures were explained with changes of constituent materials, geometric parameters of nanostructure, thermal loads and hydro-genation process. It was concluded that manufacturing the novel nanocomposite structures made of graphene origami offers a novel controllable structure for application in special condition and desired purposes. The responses of graphene origami reinforced structures subjected to mechanical and thermal loads leads to interesting outputs in both static and dynamic problems that encourage readers for further investigation. It is concluded that employing these materials leads to a controllable and tuneable material and structure in thermal environment. The static bending results of a composite cylindrical shell composed of copper matrix reinforced with G-Ori are presented in this paper.

2. Formulation

The static bending results of a shear deformable cylindrical panel is studied in this section using a shear deformable model. The structure is assumed composed of a copper based matric reinforced with distribution of graphene origami.

The foldability-dependent constitutive relations for a cylindrical panel are extended with accounting the thermal strain as follows (Arefi *et al*. 2020, Bidgoli and Arefi 2023, Addou *et al*. 2023, Luo *et al*. 2024):

$$\begin{Bmatrix} \sigma_{xx} \\ \sigma_{\theta\theta} \\ \tau_{x\theta} \\ \tau_{z\theta} \\ \tau_{xz} \end{Bmatrix} = \frac{E_{eff}}{\left(1-\nu_{eff}^2\right)} \begin{bmatrix} 1 & \nu_{eff} & & 0 & 0 & 0 \\ \nu_{eff} & 1 & & 0 & 0 & 0 \\ & & \frac{1-\nu_{eff}}{2} & 0 & & \\ 0 & 0 & & \frac{1-\nu_{eff}}{2} & 0 & \\ 0 & 0 & 0 & & \frac{1-\nu_{eff}}{2} & \\ 0 & 0 & 0 & & & \end{bmatrix} \begin{Bmatrix} \varepsilon_{xx}-\alpha_{eff}T \\ \varepsilon_{\theta\theta}-\alpha_{eff}T \\ \gamma_{xt} \\ \gamma_{zt} \\ \gamma_{xz} \end{Bmatrix} \tag{1}$$

In which σ_{ij}, $\tau_{ij}, \varepsilon_{xx}$, γ_{xt} are stress and strain components. Furthermore E_{eff}, ν_{eff} are effective modulus of elasticity and Poisson's ratio, respectively. The shell structure is subjected to uniform temperature rising. Furthermore, the foldability/thermal/volume fraction dependent relations for effective modulus of elasticity, Poisson's ratio, and heat expansion coefficients are assumed as follows:

$$E = E_{Cu}\begin{Bmatrix}1.11-1.22V_{G.O}-0.134\,T/T_0\\+0.559V_{G.O}\,T/T_0-5.5V_{G.O}H_{Gr}\\+38V_{G.O}^2H_{G.O}-20.6V_{G.O}^2H_{G.O}^2\end{Bmatrix}\frac{\begin{pmatrix}1+2(l_{Gr}/t_{Gr})\,(E_{Gr}/E_{Cu}-1)/(E_{Gr}/E_{Cu}+2\,l_{Gr}/t_{Gr})\\W_{Gr}/\left(W_{Gr}+\rho_{Gr}/\rho_{Cu}\,(1-W_{Gr})\right)\end{pmatrix}}{(1-(E_{Gr}/E_{Cu}-1)/(E_{Gr}/E_{Cu}+\xi)\,V_{G.O})},$$

$$\nu = \{1.01-1.43V_{G.O}+0.165\,T/T_0-1.1V_{Gr}H_{Gr}\,T/T_0 - 16.8V_{G.O}H_{G.O}+16V_{G.O}^2H_{G.O}^2\}\left(\nu_{Gr}\,W_{Gr}/\left(W_{Gr}+\rho_{Gr}/\rho_{Cu}\,(1-W_{Gr})\right)+\nu_{Cu}(1-V_{Gr})\right), \quad (2)$$

$$\alpha = \left(\alpha_{Gr}\,W_{Gr}/\left(W_{Gr}+\rho_{Gr}/\rho_{Cu}\,(1-W_{Gr})\right) + \alpha_{Cu}(1-V_{G.O})\right)\{0.794-16.8V_{G.O}^2-0.0279(T/T_0)^2 + 0.182(1+V_{G.O})(T/T_0)\},$$

in which, $V_{G.O} = W_{Gr}/\left(W_{Gr}+\rho_{Gr}/\rho_{Cu}\,(1-W_{Gr})\right)$, $V_{Cu} = (1-V_{G.O})$. Furthermore, it is assumed that the reinforcements are distributed uniformly along the thickness direction. The environment and local temperatures are assumed as T, T_0 respectively. It is assumed that the shell is shear deformable and the deformations are changed linearly along the thickness direction. The shear deformability kinematic relations are extended in the cylindrical coordinate as follows (Luo and Dong 2024, Meng *et al*. 2018, 2019, 2023, 2024):

$$\begin{aligned}u(x,\theta,z) &= u_0(x,\theta)+z\varphi_x(x,\theta),\\ v(x,\theta,z) &= v_0(x,\theta)+z\varphi_\theta(x,\theta),\\ w(x,\theta,z) &= w(x,\theta)\end{aligned} \quad (3)$$

The geometric linear strain-displacement relations for small deformation yields strain components as follows:

$$\begin{aligned}\varepsilon_z &= w_{,z}, \quad \varepsilon_\theta = w/r+v_{,\theta}/r, \quad \varepsilon_x = u_{,x},\\ \gamma_{xt} &= v_{,x}+u_{,\theta}/r, \quad \gamma_{zt} = w_{,\theta}/r+v_{,z}-v/r,\\ \gamma_{xz} &= w_{,x}+u_{,z},\end{aligned} \quad (4)$$

Substitution of Eq.1 into Eq.2 gives strain components as follows (Zhang *et al*. 2024 b, c, d):

$$\begin{aligned}\varepsilon_x &= u_{0,x}+z\varphi_{x,x},\\ \varepsilon_\theta &= v_{0,\theta}/r+z\varphi_{\theta,\theta}/r+w/r,\\ \varepsilon_z &= 0,\\ \gamma_{x\theta} &= v_{0,x}+z\varphi_{\theta,x}+u_{0,\theta}/r+z\,\varphi_{x,\theta}/r,\\ \gamma_{z\theta} &= w_{,\theta}/r+\varphi_\theta-v_0/r-z\,\varphi_\theta/r,\\ \gamma_{xz} &= w_{,x}+\varphi_x,\end{aligned} \quad (5)$$

Variation of strain energy is computed with definition of resultant components as follows (Tlidji *et al*. 2022, Madenci *et al*. 2023, Xin *et al*. 2024, Xie *et al*. 2024)

$$\delta U = \int_\theta\int_x \begin{pmatrix}N_x u_{0,x}+M_x\varphi_{x,x}+N_\theta v_{0,\theta}+M_\theta\varphi_{\theta,\theta}\\+N_\theta w+N_{x\theta}v_{0,x}+M_{x\theta}\varphi_{\theta,x}+P_{x\theta}u_{0,\theta}\\+S_{x\theta}\varphi_{x,\theta}+P_{z\theta}w_{,\theta}+N_{z\theta}\varphi_\theta-P_{z\theta}v_0\\-S_{z\theta}\varphi_\theta+N_{xz}w_{,x}+N_{xz}\varphi_x\end{pmatrix}d\theta dx \quad (6)$$

Using definition of various multi-field resultant components as presented below (Bidgoli and Arefi 2022, 2023a, b, c, d, Arefi *et al*. 2018, 2019, 2021, 2022, Arefi and Bidgoli 2019, Zhang *et al*. 2023b, Adab *et al*. 2022, Arefi and Zenkour 2016 a, b, 2017, 2018, 2019, Arefi *et al*. 2012, 2016, Arefi 2016, 2018, Arefi and Rahimi 2010, 2012, Mohammadimehr *et al*. 2016, Arefi and Allam 2015):

$$\begin{aligned}\{N_x,M_x,S_x\} &= \int_{-\frac{h}{2}}^{\frac{h}{2}} r\sigma_x\{1,z\}\mathrm{d}z,\\ \{N_\theta,M_\theta\} &= \int_{-\frac{h}{2}}^{\frac{h}{2}} \sigma_\theta r\{1/r,z/r\}\mathrm{d}z,\\ \{N_{xz}\} &= \int_{-\frac{h}{2}}^{\frac{h}{2}} r\sigma_{xz}\mathrm{d}z,\\ \{N_{x\theta},M_{x\theta},P_{x\theta},S_{x\theta}\} &= \int_{-\frac{h}{2}}^{\frac{h}{2}} \sigma_{x\theta} r\{1,z,1/r,z/r\}\mathrm{d}z,\\ \{N_{z\theta},P_{z\theta},S_{z\theta}\} &= \int_{-\frac{h}{2}}^{\frac{h}{2}} \sigma_{z\theta} r\{1,1/r,z/r\}\mathrm{d}z,\end{aligned} \quad (7)$$

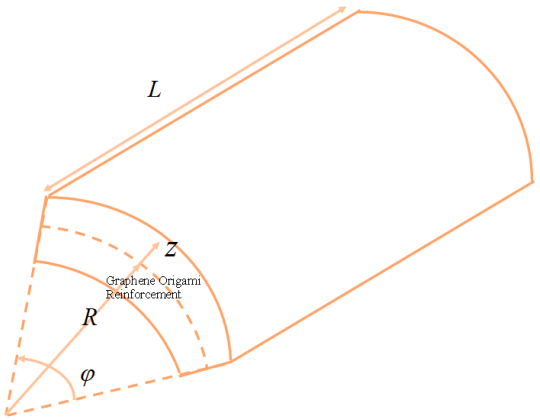

Fig. 1 The schematic figure of the graphene origami reinforced panel

The schematic figure of the problem is presented in Fig. 1 (Gong *et al*. 2024, Yu *et al*. 2024, Gao *et al*. 2024, Lu *et al*. 2025, Shi *et al*. 2025).

One can arrive at the variation in strain energy as follows (Sekkak *et al*. 2024, Shen *et al*. 2024, Sun *et al*. 2024, Zhao *et al*. 2024):

$$\delta U = \int_\theta\int_x \begin{pmatrix}-N_{x,x}\delta u_0-P_{x\theta,\theta}\delta u_0+N_{xz}\delta\varphi_x\\-M_{x,x}\delta\varphi_x-S_{x\theta,\theta}\delta\varphi_x-N_{\theta,\theta}\delta v_0\\-N_{x\theta,x}\delta v_0-P_{z\theta}\delta v_0-M_{\theta,\theta}\delta\varphi_\theta\\-M_{x\theta,x}\delta\varphi_\theta+N_{z\theta}\delta\varphi_\theta-S_{z\theta}\delta\varphi_\theta\\+N_\theta\delta w-P_{z\theta,\theta}\delta w-N_{xz,x}\delta w\end{pmatrix}d\theta dx \quad (8)$$

The structure is subjected to uniform loading, thermal and mechanical loads. The external work of initial multi-field loading is assumed as (Zhang *et al*. 2021a, b, 20222a, b, 2024a):

$$\delta W = \int\{q-\overline{N_x}w_{,x,x}-\overline{N_\theta}\,w_{,\theta,\theta}/R^2\}\delta w R dx d\theta \quad (9)$$

in which $\overline{N_x} = \left(N_{x_0}^{Mech}+N_{x_0}^{Therm}\right)$, $\overline{N_\theta} = \left(N_{\theta_0}^{Mech}+N_{\theta_0}^{Therm}\right)$. Using Hamilton's principle, the governing equations are derived as follows (Zhang and Zhuang 2018a, b, 2019, Zhang and Meng 2020, Zhang 2017):

$$\begin{gathered}\delta u_0: N_{x,x}+P_{x\theta,\theta}=0,\\ \delta\varphi_x: M_{x,x}+S_{x\theta,\theta}-N_{xz}=0,\\ \delta v_0: N_{\theta,\theta}+N_{x\theta,x}+P_{z\theta}=0\\ \delta\varphi_\theta: M_{\theta,\theta}+M_{x\theta,x}+S_{z\theta}-N_{z\theta}=0\\ \delta w: N_\theta-P_{z\theta,\theta}-N_{xz,x}+\overline{N_x}w_{,x,x}+\overline{N_\theta}\,w_{,\theta,\theta}/R^2=q,\end{gathered}\tag{10}$$

Furthermore, we will have (Peng *et al*. 2024b, Xiao *et al*. 2024a, b, Xu *et al*. 2024a, b)

$$\begin{gathered}N_x=\mathcal{L}_1u_{0,x}+\mathcal{L}_2\varphi_{x,x}+\mathcal{L}_3v_{0,\theta}+\mathcal{L}_4\varphi_{\theta,\theta}+\mathcal{L}_3w-\mathcal{L}_1^T\\ M_x=\mathcal{L}_5u_{0,x}+\mathcal{L}_6\varphi_{x,x}+\mathcal{L}_7v_{0,\theta}+\mathcal{L}_8\varphi_{\theta,\theta}+\mathcal{L}_7w-\mathcal{L}_2^T\\ N_{\theta\theta}=\mathcal{L}_9v_{0,\theta}+\mathcal{L}_{10}\varphi_{\theta,\theta}+\mathcal{L}_9w+\mathcal{L}_{11}u_{0,x}+\mathcal{L}_{12}\varphi_{x,x}-\mathcal{L}_3^T,\\ M_{\theta\theta}=\mathcal{L}_{13}v_{0,\theta}+\mathcal{L}_{14}\varphi_{\theta,\theta}+\mathcal{L}_{13}w\\ +\mathcal{L}_{15}u_{0,x}+\mathcal{L}_{16}\varphi_{x,x}-\mathcal{L}_4^T,\\ N_{xz}=\mathcal{L}_{17}\left(w_{,x}+\varphi_x\right)\\ N_{x\theta}=\mathcal{L}_{18}v_{0,x}+\mathcal{L}_{19}\varphi_{\theta,x}+\mathcal{L}_{20}u_{0,\theta}+\mathcal{L}_{21}\varphi_{x,\theta}\\ M_{x\theta}=\mathcal{L}_{22}v_{0,x}+\mathcal{L}_{23}\varphi_{\theta,x}+\mathcal{L}_{24}u_{0,\theta}+\mathcal{L}_{25}\varphi_{x,\theta}\\ P_{x\theta}=\mathcal{L}_{26}v_{0,x}+\mathcal{L}_{27}\varphi_{\theta,x}+\mathcal{L}_{28}u_{0,\theta}+\mathcal{L}_{29}\varphi_{x,\theta}\\ S_{x\theta}=\mathcal{L}_{30}v_{0,x}+\mathcal{L}_{31}\varphi_{\theta,x}+\mathcal{L}_{32}u_{0,\theta}+\mathcal{L}_{33}\varphi_{x,\theta}\\ N_{z\theta}=\mathcal{L}_{35}w_{,\theta}+\mathcal{L}_{34}\varphi_\theta-\mathcal{L}_{35}v_0-\mathcal{L}_{36}\varphi_\theta\\ P_{z\theta}=\mathcal{L}_{38}w_{,\theta}+\mathcal{L}_{37}\varphi_\theta-\mathcal{L}_{38}v_0-\mathcal{L}_{39}\varphi_\theta\\ S_{z\theta}=\mathcal{L}_{41}w_{,\theta}+\mathcal{L}_{40}\varphi_\theta-\mathcal{L}_{41}v_0-\mathcal{L}_{42}\varphi_\theta\end{gathered}\tag{11}$$

In which the integration constants are defined as follows (Xue *et al*. 2024, Ling *et al*. 2024, Liang *et al*. 2024b, Xinde *et al*. 2024, Huang *et al*. 2024c)

$$\begin{gathered}\{\mathcal{L}_1,\mathcal{L}_2\}=\int_{-\frac{h}{2}}^{\frac{h}{2}}\frac{rE_{eff}}{\left(1-\nu_{eff}^2\right)}\{1,z\}\mathrm{d}z,\\ \{\mathcal{L}_3,\mathcal{L}_4\}=\int_{-\frac{h}{2}}^{\frac{h}{2}}\frac{rE_{eff}\nu_{eff}}{\left(1-\nu_{eff}^2\right)}\{1/r\,,z/r\}\mathrm{d}z,\\ \mathcal{L}_1^T=\int_{-\frac{h}{2}}^{\frac{h}{2}}r\alpha_{eff}\left(1+\nu_{eff}\right)T\mathrm{d}z\\ \{\mathcal{L}_5,\mathcal{L}_6\}=\int_{-\frac{h}{2}}^{\frac{h}{2}}\frac{zrE_{eff}}{\left(1-\nu_{eff}^2\right)}\{1,z\}\mathrm{d}z,\\ \{\mathcal{L}_7,\mathcal{L}_8\}=\int_{-\frac{h}{2}}^{\frac{h}{2}}\frac{zrE_{eff}\nu_{eff}}{\left(1-\nu_{eff}^2\right)}\{1/r\,,z/r\}\mathrm{d}z,\\ \mathcal{L}_2^T=\int_{-\frac{h}{2}}^{\frac{h}{2}}zr\alpha_{eff}\left(1+\nu_{eff}\right)T\mathrm{d}z\\ \{\mathcal{L}_9,\mathcal{L}_{10}\}=\int_{-\frac{h}{2}}^{\frac{h}{2}}\frac{E_{eff}}{\left(1-\nu_{eff}^2\right)}\{1/r\,,z/r\}\mathrm{d}z,\\ \{\mathcal{L}_{11},\mathcal{L}_{12}\}=\int_{-\frac{h}{2}}^{\frac{h}{2}}\frac{\nu_{eff}E_{eff}}{\left(1-\nu_{eff}^2\right)}\{1,z\}\mathrm{d}z,\\ \mathcal{L}_3^T=\int_{-\frac{h}{2}}^{\frac{h}{2}}\alpha_{eff}\left(1+\nu_{eff}\right)T\mathrm{d}z\\ \{\mathcal{L}_{13},\mathcal{L}_{14}\}=\int_{-\frac{h}{2}}^{\frac{h}{2}}\frac{zE_{eff}}{\left(1-\nu_{eff}^2\right)}\{1/r\,,z/r\}\mathrm{d}z,\\ \{\mathcal{L}_{15},\mathcal{L}_{16}\}=\int_{-\frac{h}{2}}^{\frac{h}{2}}\frac{zE_{eff}\nu_{eff}}{\left(1-\nu_{eff}^2\right)}\{1,z\}\mathrm{d}z,\end{gathered}\tag{12}$$

$$\begin{gathered}\mathcal{L}_4^T=\int_{-\frac{h}{2}}^{\frac{h}{2}}z\alpha_{eff}\left(1+\nu_{eff}\right)T\mathrm{d}z\\ \{\mathcal{L}_{17}\}=\int_{-\frac{h}{2}}^{\frac{h}{2}}\frac{rE_{eff}}{2\left(1+\nu_{eff}\right)}\mathrm{d}z,\\ \{\mathcal{L}_{18},\mathcal{L}_{19},\mathcal{L}_{20},\mathcal{L}_{21}\}=\int_{-\frac{h}{2}}^{\frac{h}{2}}\frac{rE_{eff}}{2\left(1+\nu_{eff}\right)}\{1,z,1/r\,,z/r\}\mathrm{d}z\\ \{\mathcal{L}_{22},\mathcal{L}_{23},\mathcal{L}_{24},\mathcal{L}_{25}\}=\int_{-\frac{h}{2}}^{\frac{h}{2}}\frac{zrE_{eff}}{2\left(1+\nu_{eff}\right)}\{1,z,1/r\,,z/r\}\mathrm{d}z,\\ \{\mathcal{L}_{26},\mathcal{L}_{27},\mathcal{L}_{28},\mathcal{L}_{29}\}=\int_{-\frac{h}{2}}^{\frac{h}{2}}\frac{E_{eff}}{2\left(1+\nu_{eff}\right)}\{1,z,1/r\,,z/r\}\mathrm{d}z\\ \{\mathcal{L}_{30},\mathcal{L}_{31},\mathcal{L}_{32},\mathcal{L}_{33}\}=\int_{-\frac{h}{2}}^{\frac{h}{2}}\frac{zE_{eff}}{2\left(1+\nu_{eff}\right)}\{1,z,1/r\,,z/r\}\mathrm{d}z,\\ \{\mathcal{L}_{34},\mathcal{L}_{35},\mathcal{L}_{36}\}=\int_{-\frac{h}{2}}^{\frac{h}{2}}\frac{rE_{eff}}{2\left(1+\nu_{eff}\right)}\{1,1/r\,,z/r\}\mathrm{d}z\\ \{\mathcal{L}_{37},\mathcal{L}_{38},\mathcal{L}_{39}\}=\int_{-\frac{h}{2}}^{\frac{h}{2}}\frac{E_{eff}}{2\left(1+\nu_{eff}\right)}\{1,1/r\,,z/r\}\mathrm{d}z,\\ \{\mathcal{L}_{40},\mathcal{L}_{41},\mathcal{L}_{42}\}=\int_{-\frac{h}{2}}^{\frac{h}{2}}\frac{zE_{eff}}{2\left(1+\nu_{eff}\right)}\{1,1/r\,,z/r\}\mathrm{d}z\end{gathered}$$

Substitution of Eq.17 into Eq.16 yields to:

$$\begin{gathered}\mathcal{L}_1u_{0,x,x}+\mathcal{L}_{28}u_{0,\theta,\theta}+\mathcal{L}_2\varphi_{x,x,x}+\mathcal{L}_{29}\varphi_{x,\theta,\theta}+\\ (\mathcal{L}_3+\mathcal{L}_{26})v_{0,x,\theta}+(\mathcal{L}_4+\mathcal{L}_{27})\varphi_{\theta,x,\theta}+\mathcal{L}_3w_{,x}-\mathcal{L}_{1,x}^T=0,\\ \mathcal{L}_5u_{0,x,x}+\mathcal{L}_{32}u_{0,\theta,\theta}+\mathcal{L}_6\varphi_{x,x,x}+\mathcal{L}_{33}\varphi_{x,\theta,\theta}-\mathcal{L}_{17}\varphi_x+\\ (\mathcal{L}_7+\mathcal{L}_{30})v_{0,x,\theta}+(\mathcal{L}_8+\mathcal{L}_{31})\varphi_{\theta,x,\theta}+(\mathcal{L}_7-\mathcal{L}_{17})w_{,x}-\mathcal{L}_{2,x}^T=0,\\ (\mathcal{L}_{11}+\mathcal{L}_{20})u_{0,\theta,x}+(\mathcal{L}_{21}+\mathcal{L}_{12})\varphi_{x,x,\theta}+\mathcal{L}_{18}v_{0,x,x}+\\ \mathcal{L}_9v_{0,\theta,\theta}-\mathcal{L}_{38}v_0+\mathcal{L}_{19}\varphi_{\theta,x,x}+\mathcal{L}_{10}\varphi_{\theta,\theta,\theta}+(\mathcal{L}_{37}-\mathcal{L}_{39})\varphi_\theta\\ +(\mathcal{L}_9+\mathcal{L}_{38})w_{,\theta}-\mathcal{L}_{3,\theta}^T=0\\ (\mathcal{L}_{15}+\mathcal{L}_{24})u_{0,\theta,x}+(\mathcal{L}_{25}+\mathcal{L}_{16})\varphi_{x,x,\theta}+\mathcal{L}_{22}v_{0,x,x}+\\ \mathcal{L}_{13}v_{0,\theta,\theta}+(\mathcal{L}_{35}-\mathcal{L}_{41})v_0+\mathcal{L}_{23}\varphi_{\theta,x,x}+\mathcal{L}_{14}\varphi_{\theta,\theta,\theta}\\ +(\mathcal{L}_{36}+\mathcal{L}_{40}-\mathcal{L}_{42}-\mathcal{L}_{34})\varphi_\theta+(\mathcal{L}_{13}+\mathcal{L}_{41}-\mathcal{L}_{35})w_{,\theta}-\mathcal{L}_{4,\theta}^T=0\\ \mathcal{L}_{11}u_{0,x}+(\mathcal{L}_{12}-\mathcal{L}_{17})\varphi_{x,x}+(\mathcal{L}_9+\mathcal{L}_{38})v_{0,\theta}+\\ (\mathcal{L}_{10}+\mathcal{L}_{39}-\mathcal{L}_{37})\varphi_{\theta,\theta}+(\overline{N_x}-\mathcal{L}_{17})w_{,x,x}\\ +(\overline{N_\theta}/R^2-\mathcal{L}_{38})w_{,\theta,\theta}+\mathcal{L}_9w-\mathcal{L}_3^T=q,\end{gathered}\tag{13}$$

3. Solution

After derivation of the governing motion's equations, one can use the trigonometric functions for satisfying of the simply supported mechanical boundary conditions as follows

$$\begin{gathered}\begin{Bmatrix}u_0\\ \varphi_x\\ v_0\\ \varphi_\theta\\ w\end{Bmatrix}=\sum_{n=1}^{\infty}\sum_{m=1}^{\infty}e^{i\omega t}\begin{Bmatrix}Ucos(\alpha_nx)sin(\beta_m\theta)\\ \emptyset_xcos(\alpha_nx)sin(\beta_m\theta)\\ Vsin(\alpha_nx)cos(\beta_m\theta)\\ \emptyset_\theta sin(\alpha_nx)cos(\beta_m\theta)\\ Wsin(\alpha_nx)sin(\beta_m\theta)\end{Bmatrix},\\ \alpha_n=\frac{n\pi}{L},\beta_m=\frac{m\pi}{\Theta}\end{gathered}\tag{14}$$

In which U, $\emptyset_x$, V, $\emptyset_\theta$, W show maximum values of displacements and rotations. The Navier's technique is applied for simply-supported boundary conditions where the edges are free to rotate at the boundaries and only the

Table 1 Comparison of the results with changes of various geometric parameters literature results (Ren 1989, Alibeigloo 2014)

	References	$L/(R\Theta)=0.5$	$L/(R\Theta)=1$	$L/(R\Theta)=1.5$	$L/(R\Theta)=2$
a/h=10	Present	1.31822	0.55465	0.40545	0.35122
	Ren (1989)	1.31631	0.55010	0.39963	0.34600
	Alibeigloo (2014)	1.31742	0.55049	0.39987	0.34600
a/h=100	Present	0.16988	0.07425	0.04922	0.03962
	Ren (1989)	0.16001	0.07301	0.04901	0.03921
	Alibeigloo (2014)	0.16066	0.07368	0.04912	0.03925

Table 2 Effect of graphene origami percent $\%V_{G.Ori}$ on the all displacement and rotation components $\overline{w}$, $\overline{v_0}$, $\overline{u_0}$, $\overline{\varphi_x}$, $\overline{\varphi_\theta}$

$\%\boldsymbol{V_{G.Ori}}$	$\overline{w}$	$\overline{v_0}$	$\overline{u_0}$	$\overline{\varphi_x}$	$\overline{\varphi_\theta}$
0	0.0091468	0.0005827	0.0000457	0.0575108	-0.7267684
0.1	0.0090541	0.0005767	0.0000452	0.0569276	-0.7193918
0.2	0.0089632	0.0005710	0.0000448	0.0563560	-0.7121631
0.3	0.0088741	0.0005653	0.0000443	0.0557958	-0.7050779
0.4	0.0087868	0.0005597	0.0000439	0.0552466	-0.6981319
0.5	0.0087012	0.0005542	0.0000435	0.0547081	-0.6913211
0.6	0.0086172	0.0005489	0.0000430	0.0541799	-0.6846417
0.7	0.0085348	0.0005436	0.0000426	0.0536619	-0.6780898
0.8	0.0084540	0.0005385	0.0000422	0.0531536	-0.6716619
0.9	0.0083747	0.0005334	0.0000418	0.0526549	-0.6653544
1	0.0082968	0.0005285	0.0000414	0.0521654	-0.6591641
1.1	0.0082204	0.0005236	0.0000411	0.0516850	-0.6530877
1.2	0.0081454	0.0005188	0.0000407	0.0512132	-0.6471220
1.3	0.0080718	0.0005141	0.0000403	0.0507501	-0.6412642
1.4	0.0079994	0.0005095	0.0000400	0.0502952	-0.6355113
1.5	0.0079284	0.0005050	0.0000396	0.0498484	-0.6298605
1.6	0.0078586	0.0005005	0.0000393	0.0494094	-0.6243092
1.7	0.0077900	0.0004962	0.0000389	0.0489781	-0.6188548
1.8	0.0077226	0.0004919	0.0000386	0.0485543	-0.6134947
1.9	0.0076564	0.0004876	0.0000382	0.0481377	-0.6082265
2	0.0075913	0.0004835	0.0000379	0.0477282	-0.6030479

transverse deflection is restrained. Substitution of the solution from Eq. 19 into Eq. 18 yields:

$$\begin{gathered}
\mathcal{L}_1 u_{0,x,x} + \mathcal{L}_{28} u_{0,\theta,\theta} + \mathcal{L}_2 \varphi_{x,x,x} + \mathcal{L}_{29} \varphi_{x,\theta,\theta} \\
+(\mathcal{L}_3 + \mathcal{L}_{26}) v_{0,x,\theta} + (\mathcal{L}_4 + \mathcal{L}_{27}) \varphi_{\theta,x,\theta} + \mathcal{L}_3 w_{,x} - \mathcal{L}^T_{1,x} = 0, \\
\mathcal{L}_5 u_{0,x,x} + \mathcal{L}_{32} u_{0,\theta,\theta} + \mathcal{L}_6 \varphi_{x,x,x} + \mathcal{L}_{33} \varphi_{x,\theta,\theta} \\
-\mathcal{L}_{17} \varphi_x + +(\mathcal{L}_7 + \mathcal{L}_{30}) v_{0,x,\theta} \\
+(\mathcal{L}_8 + \mathcal{L}_{31}) \varphi_{\theta,x,\theta} + (\mathcal{L}_7 - \mathcal{L}_{17}) w_{,x} - \mathcal{L}^T_{2,x} = 0 \\
(\mathcal{L}_{11} + \mathcal{L}_{20}) u_{0,\theta,x} + (\mathcal{L}_{21} + \mathcal{L}_{12}) \varphi_{x,x,\theta} + \mathcal{L}_{18} v_{0,x,x} + \\
+\mathcal{L}_9 v_{0,\theta,\theta} - \mathcal{L}_{38} v_0 + \mathcal{L}_{19} \varphi_{\theta,x,x} + \mathcal{L}_{10} \varphi_{\theta,\theta,\theta} \\
+(\mathcal{L}_{37} - \mathcal{L}_{39}) \varphi_\theta + (\mathcal{L}_9 + \mathcal{L}_{38}) w_{,\theta} - \mathcal{L}^T_{3,\theta} = 0 \\
(\mathcal{L}_{15} + \mathcal{L}_{24}) u_{0,\theta,x} + (\mathcal{L}_{25} + \mathcal{L}_{16}) \varphi_{x,x,\theta} + \mathcal{L}_{22} v_{0,x,x} + \mathcal{L}_{13} v_{0,\theta,\theta} \\
+(\mathcal{L}_{35} - \mathcal{L}_{41}) v_0 + (\mathcal{L}_{36} + \mathcal{L}_{40} - \mathcal{L}_{42} - \mathcal{L}_{34}) \varphi_\theta \\
+\mathcal{L}_{23} \varphi_{\theta,x,x} + \mathcal{L}_{14} \varphi_{\theta,\theta,\theta} (\mathcal{L}_{13} + \mathcal{L}_{41} - \mathcal{L}_{35}) w_{,\theta} - \mathcal{L}^T_{4,\theta} = 0 \\
\mathcal{L}_{11} u_{0,x} + (\mathcal{L}_{12} - \mathcal{L}_{17}) \varphi_{x,x} + (\mathcal{L}_9 + \mathcal{L}_{38}) v_{0,\theta} \\
+(\mathcal{L}_{10} + \mathcal{L}_{39} - \mathcal{L}_{37}) \varphi_{\theta,\theta} + (\overline{N_x} - \mathcal{L}_{17}) w_{,x,x} \\
+(\overline{N_\theta}/R^2 - \mathcal{L}_{38}) w_{,\theta,\theta} + \mathcal{L}_9 w - \mathcal{L}^T_3 = q,
\end{gathered} \tag{15}$$

Or in compact form, one can arrive at more simple form as follows:

$$[K]\{X\} = \{F\}, \tag{16}$$

In order to verify the formulation and solution procedure, a comparative study is presented in this section. This comparison is done using comparison with References (Ren 1989, Alibeigloo 2014) with changes of various geometric parameters.

To present a comprehensive investigation on the effect of graphene origami percent $\%V_{G.Ori}$ on the all displacement and rotation components $\overline{w}, \overline{v_0}, \overline{u_0}, \overline{\varphi_x}, \overline{\varphi_\theta}$, Table 2 lists variation in all mentioned components with changes of graphene origami percent $\%V_{G.Ori}$. It shows that among three displacement components, the transverse deflection is dominant and between in-plane displacements, the circumferential displacement is more than axial one. Furthermore,

Table 3 Effect of graphene origami percent $\%V_{G.Ori}$ on the dimensional axial displacement $\overline{u_0}$

$\%V_{G.Ori}$	z=-0.0005	z=-0.00025	z=0	z=0.00025	z=0.0005
0	0.0000169	0.0000313	0.0000457	0.0000601	0.0000744
0.1	0.0000168	0.0000310	0.0000452	0.0000595	0.0000737
0.2	0.0000166	0.0000307	0.0000448	0.0000589	0.0000729
0.3	0.0000164	0.0000304	0.0000443	0.0000583	0.0000722
0.4	0.0000163	0.0000301	0.0000439	0.0000577	0.0000715
0.5	0.0000161	0.0000298	0.0000435	0.0000571	0.0000708
0.6	0.0000159	0.0000295	0.0000430	0.0000566	0.0000701
0.7	0.0000158	0.0000292	0.0000426	0.0000560	0.0000695
0.8	0.0000156	0.0000289	0.0000422	0.0000555	0.0000688
0.9	0.0000155	0.0000287	0.0000418	0.0000550	0.0000682
1	0.0000154	0.0000284	0.0000414	0.0000545	0.0000675
1.1	0.0000152	0.0000281	0.0000411	0.0000540	0.0000669
1.2	0.0000151	0.0000279	0.0000407	0.0000535	0.0000663
1.3	0.0000149	0.0000276	0.0000403	0.0000530	0.0000657
1.4	0.0000148	0.0000274	0.0000400	0.0000525	0.0000651
1.5	0.0000147	0.0000271	0.0000396	0.0000521	0.0000645
1.6	0.0000145	0.0000269	0.0000393	0.0000516	0.0000640
1.7	0.0000144	0.0000267	0.0000389	0.0000512	0.0000634
1.8	0.0000143	0.0000264	0.0000386	0.0000507	0.0000629
1.9	0.0000142	0.0000262	0.0000382	0.0000503	0.0000623
2	0.0000141	0.0000260	0.0000379	0.0000499	0.0000618

Table 4 Effect of graphene origami percent $\%V_{G.Ori}$ on the dimensional axial displacement $\overline{v_0}$

$\%V_{G.Ori}$	z=-0.0005	z=-0.00025	z=0	z=0.00025	z=0.0005
0	0.0002193	0.0004010	0.0005827	0.0007644	0.0009460
0.1	0.0002171	0.0003969	0.0005767	0.0007566	0.0009364
0.2	0.0002149	0.0003929	0.0005710	0.0007490	0.0009270
0.3	0.0002127	0.0003890	0.0005653	0.0007415	0.0009178
0.4	0.0002106	0.0003852	0.0005597	0.0007342	0.0009088
0.5	0.0002086	0.0003814	0.0005542	0.0007271	0.0008999
0.6	0.0002066	0.0003777	0.0005489	0.0007201	0.0008912
0.7	0.0002046	0.0003741	0.0005436	0.0007132	0.0008827
0.8	0.0002027	0.0003706	0.0005385	0.0007064	0.0008743
0.9	0.0002008	0.0003671	0.0005334	0.0006998	0.0008661
1	0.0001989	0.0003637	0.0005285	0.0006933	0.0008581
1.1	0.0001971	0.0003603	0.0005236	0.0006869	0.0008501
1.2	0.0001953	0.0003570	0.0005188	0.0006806	0.0008424
1.3	0.0001935	0.0003538	0.0005141	0.0006744	0.0008348
1.4	0.0001918	0.0003506	0.0005095	0.0006684	0.0008273
1.5	0.0001901	0.0003475	0.0005050	0.0006625	0.0008199
1.6	0.0001884	0.0003445	0.0005005	0.0006566	0.0008127
1.7	0.0001867	0.0003415	0.0004962	0.0006509	0.0008056
1.8	0.0001851	0.0003385	0.0004919	0.0006452	0.0007986
1.9	0.0001835	0.0003356	0.0004876	0.0006397	0.0007918
2	0.0001820	0.0003327	0.0004835	0.0006343	0.0007850

Table 5 Effect of graphene origami percent $\%V_{G.Ori}$ on the axial strain e_{xx}

$\%V_{G.Ori}$	z=-0.0005	z=-0.00025	z=0	z=0.00025	z=0.0005
0	0.000848194	0.000280585	-0.00028702	0.000280585	0.000848194
0.1	0.000839589	0.000277737	-0.00028411	0.000277737	0.000839589
0.2	0.000831156	0.000274946	-0.00028127	0.000274946	0.000831156
0.3	0.000822891	0.00027221	-0.00027847	0.00027221	0.000822891
0.4	0.000814789	0.000269528	-0.00027573	0.000269528	0.000814789
0.5	0.000806844	0.000266898	-0.00027305	0.000266898	0.000806844
0.6	0.000799052	0.000264318	-0.00027042	0.000264318	0.000799052
0.7	0.000791409	0.000261788	-0.00026783	0.000261788	0.000791409
0.8	0.00078391	0.000259306	-0.0002653	0.000259306	0.00078391
0.9	0.000776553	0.00025687	-0.00026281	0.00025687	0.000776553
1	0.000769331	0.00025448	-0.00026037	0.00025448	0.000769331
1.1	0.000762243	0.000252134	-0.00025798	0.000252134	0.000762243
1.2	0.000755284	0.00024983	-0.00025562	0.00024983	0.000755284
1.3	0.00074845	0.000247568	-0.00025331	0.000247568	0.00074845
1.4	0.000741739	0.000245346	-0.00025105	0.000245346	0.000741739
1.5	0.000735147	0.000243164	-0.00024882	0.000243164	0.000735147
1.6	0.000728671	0.000241021	-0.00024663	0.000241021	0.000728671
1.7	0.000722308	0.000238914	-0.00024448	0.000238914	0.000722308
1.8	0.000716055	0.000236845	-0.00024237	0.000236845	0.000716055
1.9	0.00070991	0.00023481	-0.00024029	0.00023481	0.00070991
2	0.000703868	0.00023281	-0.00023825	0.00023281	0.000703868

Table 6 Effect of graphene origami percent $\%V_{G.Ori}$ on the axial strain e_{tt}

$\%V_{G.Ori}$	z=-0.0005	z=-0.00025	z=0	z=0.00025	z=0.0005
0	-0.000848194	-0.000280585	0.000287023	0.000854631	0.001422239
0.1	-0.000839589	-0.000277737	0.000284115	0.000845967	0.001407818
0.2	-0.000831156	-0.000274946	0.000281265	0.000837476	0.001393686
0.3	-0.000822891	-0.00027221	0.000278472	0.000829153	0.001379835
0.4	-0.000814789	-0.000269528	0.000275734	0.000820995	0.001366256
0.5	-0.000806844	-0.000266898	0.000273049	0.000812995	0.001352941
0.6	-0.000799052	-0.000264318	0.000270415	0.000805149	0.001339882
0.7	-0.000791409	-0.000261788	0.000267832	0.000797453	0.001327073
0.8	-0.00078391	-0.000259306	0.000265298	0.000789903	0.001314507
0.9	-0.000776553	-0.00025687	0.000262812	0.000782494	0.001302176
1	-0.000769331	-0.00025448	0.000260371	0.000775222	0.001290073
1.1	-0.000762243	-0.000252134	0.000257976	0.000768085	0.001278194
1.2	-0.000755284	-0.00024983	0.000255624	0.000761077	0.001266531
1.3	-0.00074845	-0.000247568	0.000253314	0.000754196	0.001255079
1.4	-0.000741739	-0.000245346	0.000251046	0.000747439	0.001243831
1.5	-0.000735147	-0.000243164	0.000248818	0.000740801	0.001232784
1.6	-0.000728671	-0.000241021	0.00024663	0.00073428	0.001221931
1.7	-0.000722308	-0.000238914	0.000244479	0.000727873	0.001211267
1.8	-0.000716055	-0.000236845	0.000242366	0.000721577	0.001200788
1.9	-0.00070991	-0.00023481	0.000240289	0.000715389	0.001190488
2	-0.000703868	-0.00023281	0.000238247	0.000709305	0.001180363

Table 7 Effect of graphene origami foldability percent $\%H_{G.Ori}$ on the dimensional axial displacement $\overline{u_0}$

$\%H_{G.Ori}$	z=-0.0005	z=-0.00025	z=0	z=0.00025	z=0.0005
0	0.00001659	0.00003068	0.00004477	0.00005887	0.00007296
5	0.00001659	0.00003069	0.00004478	0.00005888	0.00007298
10	0.00001660	0.00003070	0.00004479	0.00005889	0.00007299
15	0.00001660	0.00003070	0.00004481	0.00005891	0.00007301
20	0.00001661	0.00003071	0.00004482	0.00005892	0.00007303
25	0.00001661	0.00003072	0.00004483	0.00005894	0.00007305
30	0.00001662	0.00003073	0.00004484	0.00005895	0.00007306
35	0.00001662	0.00003074	0.00004485	0.00005897	0.00007308
40	0.00001662	0.00003074	0.00004486	0.00005898	0.00007310
45	0.00001663	0.00003075	0.00004487	0.00005900	0.00007312
50	0.00001664	0.00003076	0.00004489	0.00005901	0.00007314
55	0.00001664	0.00003077	0.00004490	0.00005903	0.00007316
60	0.00001665	0.00003078	0.00004491	0.00005904	0.00007318
65	0.00001665	0.00003079	0.00004492	0.00005906	0.00007320
70	0.00001666	0.00003080	0.00004494	0.00005908	0.00007322
75	0.00001666	0.00003081	0.00004495	0.00005909	0.00007324
80	0.00001667	0.00003081	0.00004496	0.00005911	0.00007326
85	0.00001667	0.00003082	0.00004498	0.00005913	0.00007328
90	0.00001668	0.00003083	0.00004499	0.00005914	0.00007330
95	0.00001668	0.00003084	0.00004500	0.00005916	0.00007332
100	0.00001669	0.00003085	0.00004502	0.00005918	0.00007334

Table 8 Effect of graphene origami foldability percent $\%H_{G.Ori}$ on the dimensional circumferential displacement $\overline{v_0}$

$\%H_{G.Ori}$	z=-0.0005	z=-0.00025	z=0	z=0.00025	z=0.0005
0	0.0002149	0.0003931	0.0005712	0.0007493	0.0009274
5	0.0002150	0.0003931	0.0005713	0.0007494	0.0009276
10	0.0002150	0.0003932	0.0005714	0.0007496	0.0009278
15	0.0002151	0.0003933	0.0005715	0.0007497	0.0009279
20	0.0002151	0.0003934	0.0005716	0.0007499	0.0009281
25	0.0002152	0.0003935	0.0005718	0.0007500	0.0009283
30	0.0002152	0.0003935	0.0005719	0.0007502	0.0009285
35	0.0002153	0.0003936	0.0005720	0.0007504	0.0009287
40	0.0002153	0.0003937	0.0005721	0.0007505	0.0009289
45	0.0002154	0.0003938	0.0005723	0.0007507	0.0009292
50	0.0002154	0.0003939	0.0005724	0.0007509	0.0009294
55	0.0002155	0.0003940	0.0005725	0.0007511	0.0009296
60	0.0002155	0.0003941	0.0005727	0.0007512	0.0009298
65	0.0002156	0.0003942	0.0005728	0.0007514	0.0009300
70	0.0002156	0.0003943	0.0005729	0.0007516	0.0009303
75	0.0002157	0.0003944	0.0005731	0.0007518	0.0009305
80	0.0002158	0.0003945	0.0005732	0.0007520	0.0009307
85	0.0002158	0.0003946	0.0005734	0.0007522	0.0009310
90	0.0002159	0.0003947	0.0005735	0.0007524	0.0009312
95	0.0002159	0.0003948	0.0005737	0.0007526	0.0009315
100	0.0002160	0.0003949	0.0005738	0.0007528	0.0009317

Table 9 Effect of graphene origami foldability percent $\%H_{G.Ori}$ on the axial strain $\overline{e_{xx}}$

$\%H_{G.Ori}$	z=-0.0005	z=-0.00025	z=0	z=0.00025	z=0.0005
0	0.0008314	0.0002751	-0.0002813	-0.0008377	-0.0013941
5	0.0008316	0.0002751	-0.0002814	-0.0008379	-0.0013944
10	0.0008318	0.0002752	-0.0002815	-0.0008381	-0.0013947
15	0.0008320	0.0002752	-0.0002815	-0.0008383	-0.0013950
20	0.0008321	0.0002753	-0.0002816	-0.0008385	-0.0013953
25	0.0008323	0.0002753	-0.0002817	-0.0008387	-0.0013956
30	0.0008325	0.0002754	-0.0002817	-0.0008388	-0.0013960
35	0.0008327	0.0002754	-0.0002818	-0.0008391	-0.0013963
40	0.0008329	0.0002755	-0.0002819	-0.0008393	-0.0013966
45	0.0008331	0.0002756	-0.0002820	-0.0008395	-0.0013970
50	0.0008333	0.0002756	-0.0002820	-0.0008397	-0.0013973
55	0.0008335	0.0002757	-0.0002821	-0.0008399	-0.0013977
60	0.0008337	0.0002757	-0.0002822	-0.0008401	-0.0013980
65	0.0008339	0.0002758	-0.0002823	-0.0008403	-0.0013984
70	0.0008341	0.0002759	-0.0002823	-0.0008406	-0.0013988
75	0.0008343	0.0002759	-0.0002824	-0.0008408	-0.0013992
80	0.0008345	0.0002760	-0.0002825	-0.0008410	-0.0013995
85	0.0008348	0.0002761	-0.0002826	-0.0008413	-0.0013999
90	0.0008350	0.0002762	-0.0002827	-0.0008415	-0.0014003
95	0.0008352	0.0002762	-0.0002828	-0.0008417	-0.0014007
100	0.0008354	0.0002763	-0.0002828	-0.0008420	-0.0014011

Table 10 Effect of graphene origami foldability percent $\%H_{G.Ori}$ on the circumferential strain $\overline{e_{tt}}$

$\%H_{G.Ori}$	z=-0.0005	z=-0.00025	z=0	z=0.00025	z=0.0005
0	-0.0281297	-0.0140320	0.0000305	0.0140579	0.0280503
5	-0.0281359	-0.0140355	0.0000297	0.0140598	0.0280549
10	-0.0281422	-0.0140390	0.0000289	0.0140617	0.0280596
15	-0.0281486	-0.0140426	0.0000281	0.0140637	0.0280643
20	-0.0281552	-0.0140463	0.0000273	0.0140658	0.0280692
25	-0.0281618	-0.0140500	0.0000265	0.0140679	0.0280742
30	-0.0281685	-0.0140538	0.0000257	0.0140700	0.0280793
35	-0.0281754	-0.0140576	0.0000249	0.0140723	0.0280846
40	-0.0281824	-0.0140615	0.0000241	0.0140745	0.0280899
45	-0.0281894	-0.0140654	0.0000233	0.0140769	0.0280954
50	-0.0281966	-0.0140694	0.0000225	0.0140792	0.0281009
55	-0.0282039	-0.0140734	0.0000217	0.0140817	0.0281066
60	-0.0282114	-0.0140776	0.0000209	0.0140842	0.0281124
65	-0.0282189	-0.0140817	0.0000201	0.0140867	0.0281183
70	-0.0282266	-0.0140859	0.0000193	0.0140894	0.0281243
75	-0.0282343	-0.0140902	0.0000185	0.0140920	0.0281304
80	-0.0282422	-0.0140946	0.0000177	0.0140948	0.0281367
85	-0.0282502	-0.0140990	0.0000169	0.0140975	0.0281431
90	-0.0282583	-0.0141034	0.0000161	0.0141004	0.0281495
95	-0.0282666	-0.0141079	0.0000153	0.0141033	0.0281561
100	-0.0282749	-0.0141125	0.0000145	0.0141063	0.0281629

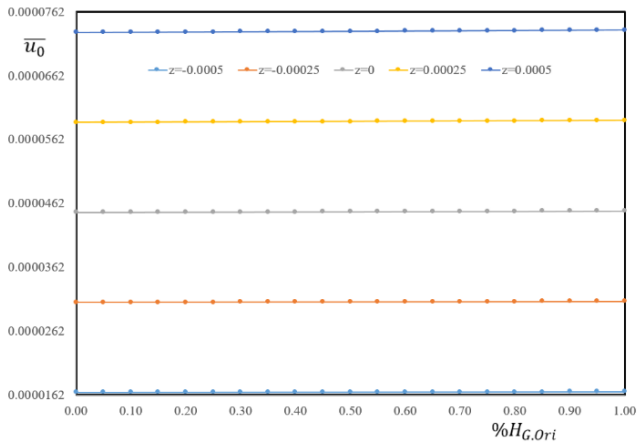

Fig. 2 Variation in dimensionless axial displacement $\overline{u_0}$ with changes of foldability parameter along the thickness direction

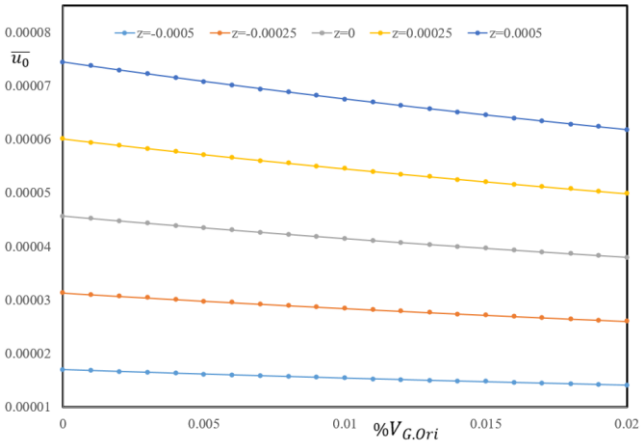

Fig. 3 Variation in dimensionless axial displacement $\overline{u_0}$ with changes of volume fraction along the thickness direction

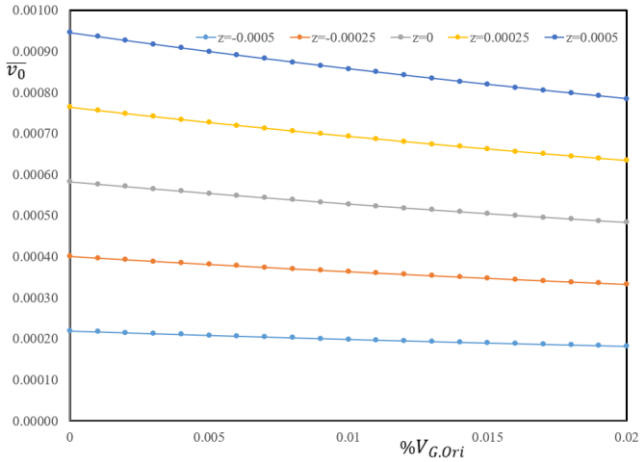

Fig. 4 Variation in dimensionless axial displacement $\overline{v_0}$ with changes of volume fraction along the thickness direction

the circumferential rotation is more than axial rotation. As a comprehensive result, it is concluded that all displacement and rotation components $\overline{w}, \overline{v_0}, \overline{u_0}, \overline{\varphi_x}, \overline{\varphi_\theta}$, are decreased with an enhancement in graphene origami percent $\%V_{G.Ori}$ because of an increase in structural stiffness.

To investigate impact of graphene origami percent $\%V_{G.Ori}$ on the dimensional axial displacement $\overline{u_0}$ at different radial coordinate, Table 3 is presented to list variation in dimensional axial displacement $\overline{u_0}$ with changes of graphene origami percent $\%V_{G.Ori}$ for different radial coordinate z=-0.0005, -0.00025, 0, 0.00025, 0.0005. The results show an enhancement in dimensional axial displacement $\overline{u_0}$ along the radial coordinate. In addition, a decrease in axial displacement is observed with an increase in graphene origami percent $\%V_{G.Ori}$.

Table 4 presents variation in dimensional circumferential displacement $\overline{v_0}$ with an enhancement in graphene origami percent $\%V_{G.Ori}$ along the various radial coordinates. One can arrive an enhancement behavior with an increase in radial coordinate.

Listed in Table 5 is variation in dimensional axial strain $\overline{e_{xx}}$ with an enhancement in graphene origami percent $\%V_{G.Ori}$ along the various radial coordinates. One can arrive an enhancement behavior with an increase in radial coordinate. It is deduced that the maximum axial strain is occurred at top/bottom surfaces while the minimum one is occurred at middle surface.

Listed in Table 6 is variation in dimensional circumferential strain $\overline{e_{tt}}$ with an enhancement in graphene origami percent $\%V_{G.Ori}$ along the various radial coordinates. It is deduced that the circumferential strain sign is changed from the inner with a compressive state to outer surfaces with a tensile state. In addition, a decrease in dimensional circumferential strain $\overline{e_{tt}}$ is observed with an enhancement in structural stiffness.

In continuation, the effect of foldability parameter $\%H_{G.Ori}$ is studied on the bending responses of the curved panel. Listed in Table 7 is variation in dimensional axial displacement $\overline{u_0}$ with an advance in radial coordinate with changes of foldability parameter $\%H_{G.Ori}$. An enhancement in dimensional axial displacement $\overline{u_0}$ is observed with an increase in foldability parameter $\%H_{G.Ori}$ because of a significant decrease in structural stiffness.

Listed in Table 8 is variation in dimensional circumferential displacement $\overline{v_0}$ with an advance in radial coordinate with changes of foldability parameter $\%H_{G.Ori}$. An enhancement in dimensional circumferential displacement $\overline{v_0}$ is observed with an increase in foldability parameter $\%H_{G.Ori}$ because of a significant decrease in structural stiffness.

Tables 9, 10 provide a detailed information on the variation in axial $\overline{e_{xx}}$ and circumferential $\overline{e_{tt}}$ strain components with an advance in foldability parameter $\%H_{G.Ori}$ along the thickness direction. It is observed that the sign of axial strain is changed from tensile to compressive from inner to outer surfaces. In addition, unlike the axial strain, the circumferential strain sign is changed from the compressive to tensile state from inner to outer surface. Some numerical results are presented in graphical form in the following. Shown in Figs. 2 is variation of axial displacement with changes of foldability parameter with various radial coordinates. It is observed an increase in radial displacement with an increase in foldability parameter because of a decrease in structural stiffness.

Shown in Figs. 3 and 4, are variation in axial and

circumferential displacement with changes of volume fraction along the thickness direction, respectively.

4. Conclusions

A vibrational-based formulation is presented in this paper to investigate impact of hydrogenation process of graphene origami reinforcement and multi-field loading on the structural vibration responses of a sandwich cylindrical panel composed of a copper matrix core reinforced with graphene origami content sandwiched by two piezoelectric/ piezomagnetic layers. To arrive at more accurate formulation and numerical results, a novel stretchable model is used. The behavioral relations are extended through employed kinematic relations and based on effective material properties of reinforced composite shell in terms of foldability parameter and graphene content of the reinforcement. Furthermore, the results are presented with changes of various mode numbers and geometric parameters of the cylindrical panel.

An investigation on the foldability parameter was performed it was deduced that the foldability parameter leads to a decrease in natural frequencies because of a decrease in structural stiffness of nanocomposite reinforced shell.

The effect of shell's curvature was studied on the vibrational responses of the composite shell. It was deduced that an increase in span angle leads to a bit decrease in natural frequencies.

An investigation on the effect of thermal loads on the vibration responses indicates that the natural frequencies are decreased with an increase in thermal loads.

An enhancement in natural frequencies is observed with an increase in initial electric and magnetic potentials.

Acknowledgement

The authors extend their appreciation to the Deanship of Research and Graduate Studies at King Khalid University for funding this work through a Large Research Project under grant number RGP2/447/45

References

Adab, N., Arefi, M. and Amabili, M. (2022), "A comprehensive vibration analysis of rotating truncated sandwich conical microshells including porous core and GPL-reinforced face-sheets", *Compos. Struct.*, **279**, 114761. https://doi.org/10.1016/j.compstruct.2021.114761

Arefi, M. (2016), "Analysis of wave in a functionally graded magneto-electro-elastic nano-rod using nonlocal elasticity model subjected to electric and magnetic potentials", *Acta. Mech.*, **227**, 2529-2542. https://doi.org/10.1007/s00707-016-1584-7

Arefi, M. (2018), "Nonlocal free vibration analysis of a doubly curved piezoelectric nano shell", *Steel. Compos. Struct.*, **27**(4), 479-493. https://doi.org/10.12989/scs.2018.27.4.479

Arefi, M. and Allam, M.N.M. (2015), "Nonlinear Responses of an Arbitrary FGP Circular Plate Resting on Foundation", *Smart. Struct. Syst.*, **16**(1), 81-100. https://doi.org/10.12989/sss.2015.16.1.081

Arefi, M. and Mohammad-Rezaei Bidgoli, E. (2019) "Electro-elastic displacement and stress analysis of the piezoelectric doubly curved shells resting on Winkler's foundation subjected to applied voltage", *Mech. Adv. Mater. Struct*, **26**(23), 1981-1994. https://doi.org/10.1080/15376494.2018.1455937

Arefi, M. and Rahimi, G.H. (2010), "Thermo elastic analysis of a functionally graded cylinder under internal pressure using first order shear deformation theory", *Sci. Res. Essays.*, **5**(12), 1442-1454. https://doi.org/10.5897/SRE.9000953

Arefi, M. and Rahimi, G.H. (2012), "Studying the nonlinear behavior of the functionally graded annular plates with piezoelectric layers as a sensor and actuator under normal pressure", *Smart. Struct. Syst.*, **9**(2), 127-143. https://doi.org/10.12989/sss.2012.9.2.127.

Arefi, M. and Zenkour, A.M. (2016a), "Free vibration, wave propagation and tension analyses of a sandwich micro/nano rod subjected to electric potential using strain gradient theory" *Mater. Res. Exp.*, **3**(11), 115704. https://doi.org/10.1088/2053-1591/3/11/115704

Arefi, M. and Zenkour, A.M. (2016b), "Employing sinusoidal shear deformation plate theory for transient analysis of three layers sandwich nanoplate integrated with piezo-magnetic face-sheets", *Smart. Mater. Struct.*, **25**, 115040. https://doi.org/10.1088/0964-1726/25/11/115040

Arefi, M. and Zenkour, A.M. (2017), "Thermo-electro-magneto-mechanical bending behavior of size-dependent sandwich piezomagnetic nanoplates", *Mech. Res. Commun.*, **84**, 27-42. https://doi.org/10.1016/j.mechrescom.2017.06.002

Arefi, M. and Zenkour, A.M. (2018), "Size-dependent electro-elastic analysis of a sandwich microbeam based on higher-order sinusoidal shear deformation theory and strain gradient theory", *J. Intel. Mater. Syst. Struct.*, **29**(7), 1394-1406. https://doi.org/10.1177/1045389X17733333

Arefi, M. and Zenkour, A.M. (2019), "Influence of magneto-electric environments on size-dependent bending results of three-layer piezomagnetic curved nanobeam based on sinusoidal shear deformation theory", *J. Sandw. Struct. Mater.*, **21**(8), 2751-2778. https://doi.org/10.1177/1099636217723186

Arefi, M., Rahimi, G.H. and Khoshgoftar, M.J. (2012), "Exact solution of a thick walled functionally graded piezoelectric cylinder under mechanical, thermal and electrical loads in the magnetic field", *Smart. Struct. Syst.*, **9**(5), 427-439. https://doi.org/10.12989/sss.2012.9.5.427

Arefi, M., Faegh, R.K. and Loghman, A. (2016), "The effect of axially variable thermal and mechanical loads on the 2D thermoelastic response of FG cylindrical shell", *J. Therm. Stress.*, **39**(12), 1539-1559. https://doi.org/10.1080/01495739.2016.1217178

Arefi, M. Mohammad-Rezaei Bidgoli, E. Zenkour, A.M. (2018), "Size-dependent free vibration and dynamic analyses of a sandwich microbeam based on higher-order sinusoidal shear deformation theory and strain gradient theory", *Smart. Struct. Syst.*, **22**(1), 27-40. https://doi.org/10.12989/sss.2018.22.1.027.

Arefi, M., Mohammad-Rezaei Bidgoli, E. and Zenkour, A.M. (2019) "Free vibration analysis of a sandwich nano-plate including FG core and piezoelectric face-sheets by considering neutral surface", *Mech. Adv. Mater. Struct*, **26**(9), 741-752. https://doi.org/10.1080/15376494.2018.1455939

Arefi, M., Lori Dehsaraji, M. and Loghman, A. (2020), "Three dimensional free vibration analysis of functionally graded nano cylindrical shell considering thickness stretching effect", *Steel. Compos. Struct.*, **34**(5), 657-670. https://doi.org/10.12989/scs.2020.34.5.657.

Arefi, M., Moghaddam, S.K., Bidgoli, E.M.R., Kiani, M. and

Civalek, O. (2021), "Analysis of graphene nanoplatelet reinforced cylindrical shell subjected to thermo-mechanical loads", *Compos. Struct.*, **255**(1), 112924. https://doi.org/10.1016/j.compstruct.2020.112924.

Arefi, M., Mohammad-Rezaei Bidgoli, E. and Civalek O. (2022), "Bending response of FG composite doubly curved nanoshells with thickness stretching via higher-order sinusoidal shear theory", *Mech. Based. Des. Struct. Mach.*, **50**(7), 2350-2378. https://doi.org/10.1080/15397734.2020.1777157

Alibeigloo, A. (2014), "Free vibration analysis of functionally graded carbon nanotube reinforced composite cylindrical panel embedded in piezoelectric layers by using theory of elasticity", *Eur. J. Mech. A Solids.*, **44**, 104-115. https://doi.org/10.1016/j.euromechsol.2013.10.002

Abouelregal, A.E., Ersoy, H. and Civalek, Ö. (2021), "Solution of Moore-Gibson-Thompson equation of an unbounded medium with a cylindrical hole", *Mathematics*, **9**, 1536. https://doi.org/10.3390/math9131536.

Babaei, H. and Eslami, M.R. (2021), "Nonlinear analysis of thermal-mechanical coupling bending of FGP infinite length cylindrical panels based on PNS and NSGT", *Appl. Math. Modell.*, **91**, 1061-1080. https://doi.org/10.1016/j.apm.2020.10.004.

Bai, B., Wang, J., Zhai, Z. and Xu, T. (2017), "The penetration processes of red mud filtrate in a porous medium by seepage", *Transp. Porous. Media.*, **117**, 207-227. https://doi.org/10.1007/s11242-017-0829-9.

Bai, B., Xu, T., Nie, Q. and Li, P. (2020), "Temperature-driven migration of heavy metal Pb2+ along with moisture movement in unsaturated soils", *Int. J. Heat. Mass. Transf.*, **153**, 119573. https://doi.org/10.1016/j.ijheatmasstransfer.2020.119573.

Bai, B., Bai, F., Li, X., Nie, Q., Jia, X. and Wu, H. (2022), "The remediation efficiency of heavy metal pollutants in water by industrial red mud particle waste", *Environ. Tech. Innov.*, **28**, 102944. https://doi.org/10.1016/j.eti.2022.102944

Bai, B., Bai, F., Nie, Q. and Jia, X. (2023a), "A high-strength red mud-fly ash geopolymer and the implications of curing temperature", *Powd. Tech.*, **416**, 118242. https://doi.org/10.1016/j.powtec.2023.118242.

Bai, B., Fan, B., Qingke, N. and Xiangxin. J. (2023b), "A high-strength red mud-fly ash geopolymer and the implications of curing temperature", *Powd. Tech.*, **416**, 118242. https://doi.org/10.1016/j.powtec.2023.118242

Bai, B., Jing, C., Fan, B., Qingke, N. and Xiangxin. J. (2024a), "Corrosion effect of acid/alkali on cementitious red mud-fly ash materials containing heavy metal residues", *Env. Tech. Innov.*, **33**, 103485. https://doi.org/10.1016/j.eti.2023.103485

Bai, B., Jing, C., Bin, Z., Liang, C. and Yongchen. Z. (2024b), "The solidification of heavy metal Pb2+-contaminated soil by enzyme-induced calcium carbonate precipitation combined with biochar", *Biochem. Eng. J.*, **212**, 109496. https://doi.org/10.1016/j.bej.2024.109496

Bai, B., Bixia, Z., Jing, C. and Hanxiang, F. (2024c), "Development of a natural inorganic diatomite curing agent on heavy metal-contaminated loess", *Phys. Chemist. Earth.*, **136**, 103790. https://doi.org/10.1016/j.pce.2024.103790

Banoqitah, E.M., Hussain, M., Khadimallah, M.A., Ghandourah, E., Yahya, A., Basha, M. and Alshoaibi, A. (2022), "A simplified directly determination of natural frequencies of CNT: Via aspect ratio", *Adv. Nano Res.*, **13**(3), 207. https://doi.org/10.12989/anr.2022.13.3.207

Bao, X., Li, J., Shen, J., Chen, X., Zhang, C. and Cui, H. (2025), "Comprehensive multivariate joint distribution model for marine soft soil based on the vine copula", *Comput. Geotech*, **177**, A, 106814. https://doi.org/10.1016/j.compgeo.2024.106814

Cui, M., Han, D., Liu, H., Li, K.C., Tang, M., Chang, C.C., Ayaz, F., Sheng, Z. and Guan, Y.L. (2024), "Secure data sharing for consortium blockchainenabled vehicular social networks," *IEEE. T. Vehic. Tech.*, 1-14. https://doi.org/10.1109/TVT.2024.3448207.

Chen, X. Feng, P. Li, X. (2024), "High reactivity of dimethyl ether activated by zeolite ferrierite within a fer cage: A prediction study", *Molecules*, **29**, 2000. https://doi.org/10.3390/molecules29092000

Culver, C.G., Dym, C.L. and Brogan, D.K. (1972), "Bending behavior of cylindrical web panels", *J. Struct. Div.*, **98**(10). https://doi.org/10.1061/JSDEAG.0003354.

Du, Y., Keller, T., Song, C., Wu, L. and Xiong, J. (2021), "Origami-inspired carbon fiber-reinforced composite sandwich materials-Fabrication and mechanical behavior", *Compos. Sci. Tech.*, **205**: 108667. https://doi.org/10.1016/j.compscitech.2021.108667.

Fan, Y. and Shen, H.S. (2022), "Non-symmetric stiffness of origami-graphene metamaterial plates", *Compos. Struct.*, **297**, 115974. https://doi.org/10.1016/j.compstruct.2022.115974.

Fu, T., Hu, X. and Yang, C. (2023), "Impact response analysis of stiffened sandwich functionally graded porous materials doubly-curved shell with re-entrant honeycomb auxetic core", *Appl. Math. Modell.*, **124**, 553-575. https://doi.org/10.1016/j.apm.2023.08.024

Fan, J., Pan, Y., Wang, H. and Song, F. (2024a), "Efficient reverse osmosis-based desalination using functionalized graphene oxide nanopores", *Appl. Surf. Sci.*, **674**, 160937. https://doi.org/10.1016/j.apsusc.2024.160937

Fan, J., Zhang, X., He, N., Song, F. and Zhang, X. (2024b), "Physical absorption and thermodynamic modeling of CO2 in new deep eutectic solvents", *J. Mole. Liq.*, **402**, 124752. https://doi.org/10.1016/j.molliq.2024.124752.

Gao, X., Dai, Y., Zhang, C., Zhang, Y., Zong, W., Zhang, W., ... and He, G. (2023), "When it's heavier: Interfacial and solvation chemistry of isotopes in aqueous electrolytes for Zn-ion Batteries", *Angew. Chem. Int. Ed.*, **62**, 16, e202300608. https://doi.org/10.1002/anie.202300608

Gao, Y. Liu, Q. Yang, Y. and Wang, K. (2024), "Latent representation discretization for unsupervised text style generation", *Inform. Proc. Manag.*, **61**(3), 103643. https://doi.org/10.1016/j.ipm.2024.103643

Gong, H., Sardans, J., Huang, H., Yan, Z., Wang, Z. and Peñuelas, J. (2024), "Global patterns and controlling factors of tree bark C : N : P stoichiometry in forest ecosystems consistent with biogeochemical niche hypothesis", *New Phytol.*, **244**(4), 1303-1314. https://doi.org/10.1111/nph.20119.

Guo, R., Qi, L. and Mo, Z. (2019), "SiO2@Graphene composite materials obtained through different methods used as substrate materials", *Silicon*, **11**, 1261-1266. https://doi.org/10.1007/s12633-018-0058-z

Guo, L., Zhao, S., Guo, Y., Yang, J. and Kitipornchai, S. (2023), "Bandgaps in functionally graded phononic crystals containing graphene origami-enabled metamaterials", *Int. J. Mech. Sci.*, **240**, 107956. https://doi.org/10.1016/j.ijmecsci.2022.107956.

Guo, S., Deng, B., Chen, C., Ke, J., Wang, J., Long, S. and Xu, K. (2024), "Seeking in ride-on-demand service: A reinforcement learning model with dynamic price prediction," *IEEE. Internet. Things. J.*, **11**(180, 29890-29910. https://doi.org/10.1109/JIOT.2024.3407119.

Han, D., Pan, N. and Li, K.C. (2022a), "A traceable and revocable ciphertext-policy attribute-based encryption scheme based on privacy protection," *IEEE. T. Depend. Sec. Comput.*, **19**(1), 316-327. https://doi.org/10.1109/TDSC.2020.2977646.

Han, D., Zhu, Y., Li, D., Liang, W., Souri, A. and Li, K.C. (2022b), "A blockchain-based auditable access control system for private data in service-centric IoT environments," *IEEE. Trans. Ind. Inform.*, **18**(5), 3530-3540.

https://doi.org/10.1109/TII.2021.3114621.
Han, D., Shi, J., Zhao, J., Wu, H., Zhou, Y., Li, L. H., Khan, M.K. and Li, K.C. (2025), "LRCN: Layer-residual Co-Attention Networks for visual question answering", *Exp. Syst. Appl.*, **263**, 125658. https://doi.org/10.1016/j.eswa.2024.125658.
Huang, B., Kang, F., Li, X. and Zhu, S. (2024a), "Underwater dam crack image generation based on unsupervised image-to-image translation", *Auto. Constr.*, **163**, 105430. https://doi.org/10.1016/j.autcon.2024.105430
Huang, J., Feng, C., Wang, X. and Zhang, Y. (2024b), "Continuous-discontinuous element method for simulating three-dimensional reinforced concrete structures", *Struct. Concr.*, Early View. https://doi.org/10.1002/suco.202300531
Huang, Z., Li, K., Jiang, Y., Jia, Z., Lv, L. and Ma, Y. (2024c), "Graph relearn network: Reducing performance variance and improving prediction accuracy of graph neural networks", *Knowl. Based Syst.*, **301**, 112311. https://doi.org/10.1016/j.knosys.2024.112311
Jam, J.E., Maleki, S. and Andakhshideh, A. (2013), "Static analysis of laminated piezoelectric cylindrical panels", *Int. J. Aer. Sci.* **2**(1), 16-28. https://doi.org/10.5923/j.aerospace.20130201.03.
Ji, X., Jiang, P., Jiang, Y., Chen, H., Wang, W., Zhong, W., Zhang, X. and Zang, D. (2023), "Toward enhanced aerosol particle adsorption in never-bursting bubble via acoustic levitation and controlled liquid compensation", *Adv. Sci.*, **10**(19), 2300049. https://doi.org/10.1002/advs.202300049
Kong, W., Fu, T. and Rabczuk, T. (2024), "Improvement of broadband low-frequency sound absorption and energy absorbing of arched curve Helmholtz resonator with negative Poisson's ratio", *Appl. Acoust.*, **221**, 110011. https://doi.org/10.1016/j.apacoust.2024.110011
Lai, Y., Zhang, T., Yin, X., Zhu, C., Du, Y., Li, Z. and Gao, J. (2024), "An antibiotic-free platform for eliminating persistent Helicobacter pylori infection without disrupting gut microbiota", *Acta. Pharm. Sin. B.*, **14**(7), 3184-3204, https://doi.org/10.1016/j.apsb.2024.03.014.
Li, Y., Li, J., Feng, C., Wen, M. and Zhang, Y. (2024a), "An interface constitutive model of plastic tensile-compressive damage under impact loading based on continuous-discontinuous framework", *Comput. Geotech.*, **173**, 106502. https://doi.org/10.1016/j.compgeo.2024.106502
Li, J., Yang, H., Gu, X., Zou, Y., Zhan, D. and Peng, J. (2024b), "Recent advances in scanning electrochemical microscopy for probing the sites in electrocatalysts, *J. Mater. Chem. A.*, **12**(30), 18733-18750, http://dx.doi.org/10.1039/D4TA01292E
Li, J., Han, D. and Weng, T.H. (2025), "A secure data storage and sharing scheme for port supply chain based on blockchain and dynamic searchable encryption", *Comput. Stand. Interf.*, **91**, 103887. https://doi.org/10.1016/j.csi.2024.103887.
Ling, W., Jing, C., Wan, J., Mao, A., Xiao, Q., Guan, J., Cheng, J., Liu, C. and E, P. (2024), "Design and construction of the near-earth space plasma simulation system of the Space Plasma Environment Research Facility", *J. Plasma. Phys.*, **90**(1), 345900101. https://doi.org/10.1017/S0022377823001460
Liang, K., Sun, P. and Wang, D. (2024a), "Quantitative analysis of deformation performance for sakew slab based on deformation energy decomposition method of triangular prism element", *Structures*, **63**, 106447. https://doi.org/10.1016/j.istruc.2024.106447
Liang, S. Gao, Y. Hu, C. Hao, A. and Qin, H. (2024b), "Efficient photon beam diffusion for directional subsurface scattering", *IEEE. T. Visual. Comput. Graph.*, Early Access. https://doi.org/10.1109/TVCG.2024.3447668.
Long, X., Li, Y., Shen, Z., Su, Y., Gu, T. and Siow, K.S. (2024), "Review of uniqueness challenge in inverse analysis of nanoindentation", *J. Manuf. Proc.*, **131**, 1897-1916. https://doi.org/10.1016/j.jmapro.2024.10.005
Lv, H., Zeng, J., Zhu, Z., Dong, S. and Li, W. (2024), "Study on prestress distribution and structural performance of heptagonal six-five-strut alternated cable dome with inner hole", *Structures*, **65**, 106724, https://doi.org/10.1016/j.istruc.2024.106724.
Lu, K. (2024), "Online distributed algorithms for online noncooperative games with stochastic cost functions: High probability bound of regrets", *IEEE. T. Auto. Cont.*, **69**(12), 8860-8867. https://doi.org/10.1109/TAC.2024.3419018.
Lu, Y. Guo, Z. Zhang, M., Zhang, M, Jiang, X. and Wang, X. (2025), "Flow-heat coupling analysis of the 1/4 symmetrical CAP1400 nuclear island loop based on the source term approach", *Annals. Nuclear. Energy.*, **211**, 110926. https://doi.org/10.1016/j.anucene.2024.110926
Luo, Y., Zhang, H., Chen, Z., Li, Q., Ye, S. and Liu, Q. (2024), "Novel multidimensional composite development for aging resistance of SBS-modified asphalt by attaching zinc oxide on expanded vermiculite", *Energy. Fuels.*, **38**(17), 16772-16781. https://doi.org/10.1021/acs.energyfuels.4c02685.
Luo, Y.X. and Dong, Y.L. (2024), "Strain measurement at up to 3000 °C based on Ultraviolet-Digital Image Correlation", *NDT E Int.*, **146**, 103155. https://doi.org/10.1016/j.ndteint.2024.103155.
Lopatin, A.V. and Morozov, E.V. (2021), "Fundamental frequency of a sandwich cylindrical panel with clamped edges", *J. Sandw. Struct. Mater.*, **23**(1), 345-364. https://doi.org/10.1177/1099636219833433
Madenci, E. Özkiliç, Y.O. Hakamy, A. and Tounsi, A. (2023), "Experimental tensile test and micro-mechanic investigation on carbon nanotube reinforced carbon fiber composite beams", *Adv. Nano. Res.*, **14**(5), 443-450. https://doi.org/10.12989/anr.2023.14.5.443.
Mohammad-Rezaei Bidgoli, E. and Arefi, M. (2022), *Innovations in Graphene-Based Polymer Composites*, Woodhead Publishing Series in Composites Science and Engineering, 521-557. https://doi.org/10.1016/B978-0-12-823789-2.00003-0.
Mohammad-Rezaei Bidgoli, E. and Arefi, M. (2023a), "Size-dependent thermomechanical critical loads of GPL-reinforced nanobeams", *Wave. Random. Complex. Med.*, 1-21. https://doi.org/10.1080/17455030.2023.2169385
Mohammad-Rezaei Bidgoli, E. and Arefi, M. (2023b), "Dynamic results of GNPRC sandwich shells", *Steel. Compos. Struct.*, **48**(3), 263-273. https://doi.org/10.12989/scs.2023.48.3.263 Full Text PDF
Mohammad-Rezaei Bidgoli, E. and Arefi, M. (2023c), "Effect of porosity and characteristics of carbon nanotube on the nonlinear characteristics of a simply-supported sandwich plate", *Arch. Civil Mech. Eng.*, **23**, 214. https://doi.org/10.1007/s43452-023-00752-1
Mohammad-Rezaei Bidgoli, E., Arefi, M. (2023d), "Nonlinear vibration analysis of sandwich plates with honeycomb core and graphene nanoplatelet-reinforced face-sheets", *Arch. Civil Mech. Eng.*, **23**, 56. https://doi.org/10.1007/s43452-022-00589-0
Mercan, K., Baltacıoglu, A.K. and Civalek, O. (2018), "Free vibration of laminated and FGM/CNT composites annular thick plates with shear deformation by discrete singular convolution method", *Compos. Struct.*, **186**, 139-153. https://doi.org/10.1016/j.compstruct.2017.12.008
Meng, F., Pang, A., Dong, X., Han, C. and Sha, X. (2018), "H∞ optimal performance design of an unstable plant under bode integral constraint", *Complexity*, **2018**(1), 4942906. https://doi.org/10.1155/2018/4942906
Meng, F. Wang, D. Yang, P. Xie, G. (2019), "Application of sum of squares method in nonlinear H∞ control for satellite attitude maneuvers", *Complexity*, **2019**(1), 5124108. https://doi.org/10.1155/2019/5124108
Meng, F., Chen, S., Zhang, W., Ou, P., Zhang, J., Chen, C. and

Song, J. (2021), "Negative Poisson's ratio in graphene Miura origami", *Mech. Mater.*, **155**, 103774. https://doi.org/10.1016/j.mechmat.2021.103774.

Meng, S., Meng, F., Chi, H., Chen, H. and Pang, A. (2023), "A robust observer based on the nonlinear descriptor systems application to estimate the state of charge of lithium-ion batteries", *J. Frank. Inst.*, **360**(16), 11397-11413. https://doi.org/10.1016/j.jfranklin.2023.08.037

Meng, S., Meng, F., Zhang, F., Li, Q., Zhang, Y. and Zemouche, A. (2024), "Observer design method for nonlinear generalized systems with nonlinear algebraic constraints with applications, *Automatica*, **162**, 111512. https://doi.org/10.1016/j.automatica.2024.111512.

Nguyen, N.V. and Phan, D.H. (2023), "Nonlinear free vibration of bi-directional functionally graded porous plates", *Thin. Wall. Struct.*, **192**, 111198. https://doi.org/10.1016/j.tws.2023.111198

Peng, X., Han, Y., Liu, G., Li, J., Yi, B., Sa, G. and Jiang, S. (2024a), "Effect of manufacturing process parameters on the compression and energy absorption properties of 4D-printed deformable honeycomb structure", *Smart. Mater. Struct.*, **33**(7), 075035. https://doi.org/10.1088/1361-665X/ad56e7

Peng, B., Chen, J., Githinji, P.B., Gul, I., Ye, Q., Chen, M., ... and Chen, Z. (2024b), "Practical guidelines for cell segmentation models under optical aberrations in microscopy", *Comput. Struct. Biotech. J.*, **26**, 23 - 39. https://doi.org/10.1016/j.csbj.2024.09.002

Pi, X., Yan, D., Xu, Y., Pan, M., Wang, Z., Chang, M. and Qi, Z. (2025), "TLRs signaling pathway regulation, antibacterial and apoptotic activity of largemouth bass ECSIT during Edwardsiella piscicida infection", *Aquaculture*, **595**(2), 741615. https://doi.org/10.1016/j.aquaculture.2024.741615.

Punera, D. and Kant, T. (2021), "An assessment of refined hierarchical kinematic models for the bending and free vibration analyses of laminated and functionally graded sandwich cylindrical panels", *J. Sandw. Struct. Mater.*, **23**(6), 2506-2546. https://doi.org/10.1177/1099636220909826.

Qu, Y., Jin, F. and Yang, J. (2021), "Stress-induced electric potential barriers in thickness-stretch deformations of a piezoelectric semiconductor plate", *Acta. Mech.*, **232**, 4533-4543. https://doi.org/10.1007/s00707-021-03059-5

Rahbar Ranji, A. and Rostami Hoseynabadi, H. (2012), "A semi-analytical technique for bending analysis of cylindrical panels with general loading and boundary conditions", *J. Mech. Sci. Tech.*, **26**, 1711-1718. https://doi.org/10.1007/s12206-012-0438-2

Ranjbar, M. and Feli, S. (2019), "Temperature-dependent analysis of axially functionally graded CNT reinforced micro-cantilever beams subjected to low velocity impact", *Mech. Adv. Mater. Struct.*, **26**(13), 1154-1168. https://doi.org/10.1080/15376494.2018.1432788

Ray, M.C. (2023), "Exact solutions of elasticity theories for static analysis of doubly curved antisymmetric angle-ply composite shells", *Mech. Adv. Mater. Struct.*, **31**(26), 7579-7593. https://doi.org/10.1080/15376494.2023.2246223

Ren, G.J. (1989), "Analysis of simply supported laminated circular cylindrical shell roofs", *Compos. Struct.*, **11**, 277-292. https://doi.org/10.1016/0263-8223(89)90092-5.

Ren, H., Xia, X., Sun, Y., Zhai, Y., Zhang, Z., Wu, J., Li, J. and Liu, M. (2024), "Electrolyte engineering for the mass exfoliation of graphene oxide across wide oxidation degrees", *J. Mater. Chem. A.*, **12**, 35, 23416-23424. http://doi.org/10.1039/D4TA02654C

Shi, J., Han, D., Chen, C. and Shen, X. (2024), "KTMN: Knowledge-driven Two-stage Modulation Network for visual question answering", *Multimed. Syst.*, **30**, 350. https://doi.org/10.1007/s00530-024-01568-6

Song, X., Han, D., Chen, C., Shen, X. and Wu, H. (2024), "Vman: visual-modified attention network for multimodal paradigms", *Vis Comput.*, 1-18. https://doi.org/10.1007/s00371-024-03563-4

Shen, Z., Dong, R., Li, J., Su, Y. and Long, X. (2024), "Determination of gradient residual stress for elastoplastic materials by nanoindentation", *J. Manufact. Proc.*, **109**, 359-366. https://doi.org/10.1016/j.jmapro.2023.10.030

Sun, X., Zhang, K., Liu, Q., Bao, M. and Chen, Y. (2024), "Harnessing domain insights: A prompt knowledge tuning method for aspect-based sentiment analysis", *Knowl. Based. Syst.*, **298**, 111975. https://doi.org/10.1016/j.knosys.2024.111975.

Singh, A. and Kumari, P., (2020), "Analytical free vibration solution for angle-ply piezolaminated plate under cylindrical bending: A piezo-elasticity approach", *Adv. Comput. Design*, **5**(1), 55-89. https://doi.org/10.12989/acd.2020.5.1.055

Shen, H.S., Reddy, J.N. and Yu, Y. (2021), "Postbuckling of doubly curved FG-GRC laminated panels subjected to lateral pressure in thermal environments", *Mech. Adv. Mater. Struct.*, **28**(3), 260-270. https://doi.org/10.1080/15376494.2018.1556827.

Sekkak, M., Zerrouki, R., Zidour, M., Tounsi, A., Bourada, M., Selim, M.M. and Saad, H.A. (2024) "Static analysis of nonlinear FG-CNT reinforced nano-composite beam resting on Winkler/Pasternak foundation", *Adv. Nano. Res.* **16**(5), 509-519. https://doi.org/10.12989/anr.2024.16.5.509.

Sobhani, E., Masoodi, A.R., Civalek, O. and Ahmadi-Pari, A.R. (2022), "Agglomerated impact of CNT vs. GNP nanofillers on hybridization of polymer matrix for vibration of coupled hemispherical-conical-conical shells", *Aer. Sci. Tech.* **120**, 107257. https://doi.org/10.1016/j.ast.2021.107257

Tlidji, Y., Benferhat, R., Daouadji, T.H., Tounsi, A., Cong Trinh, L. (2022), "Free vibration analysis of FGP nanobeams with classical and non-classical boundary conditions using State-space approach", *Adv. Nano. Res.* **13**(5), 453-463 DOI: https://doi.org/10.12989/anr.2022.13.5.453.

Taj, M. Khadimallah, M.A. Ahmad, M. Hussain, M. Azrar, L. Safeer, M. Ayed, H. Ghandourah, E. and Mouldi, A. (2024), "Nonlocal orthotropic shell model for buckling of microtubules embedded within elastic medium", *Adv. Nano. Res.*, **17**(5), 401-408, https://doi.org/10.12989/anr.2024.17.5.401.

Tornabene, F. (2016), "General higher-order layer-wise theory for free vibrations of doubly-curved laminated composite shells and panels", *Mech. Adv. Mater. Struct.*, **23**(9), 1046-1067. https://doi.org/10.1080/15376494.2015.1121522

Thai, H.T. and Choi, D.H. (2014), "Improved refined plate theory accounting for effect of thickness stretching in functionally graded plates", *Compos. Part B: Eng.*, **56**, 705-716. https://doi.org/10.1016/j.compositesb.2013.09.008.

Vali, H. and Arefi, M. (2023), "Extension of a novel higher order modeling to the vibration responses of sandwich graphene origami cylindrical panel", *Arch. Civil. Mech. Eng.*, **23**, 268. https://doi.org/10.1007/s43452-023-00797-2

Wang, C., Su, J. and Liu, T. (2023a), "A sustainable strategy to transform cotton waste into renewable cellulose fiber self-reinforcing composite paper", *J. Clean. Prod.*, **429**, 139567. https://doi.org/10.1016/j.jclepro.2023.139567

Wang, K., Boonpratatong, A., Chen, W., Ren, L., Wei, G., Qian, Z., Zhao, D. (2023b), "The fundamental property of human leg during walking: Linearity and nonlinearity", *IEEE. T. Neural. Syst. Rehab. Eng.*, **31**, 4871-4881. https://doi.org/10.1109/TNSRE.2023.3339801

Wang, Z., Yuan, Y., Zhang, S., Lin, Y. and Tan, J. (2024a), "A multi-state fusion informer integrating transfer learning for metal tube bending early wrinkling prediction", *Appl. Soft. Comput.*, **151**, 110991. https://doi.org/10.1016/j.asoc.2023.110991

Wang, Y., Wang, J., Cai, R., Zhang, J., Xia, S., Li, Z., Yu, C., Wu,

J., Wang, P and Wu, Y. (2024b), "Enhanced local CO coverage on cu quantum dots for boosting electrocatalytic CO2 reduction to ethylene", *Adv. Funct. Mater.*, 2417764. https://doi.org/10.1002/adfm.202417764.

Wang, Z. Liao, Z. Zhou, B. Yu G. Luo, W. (2024c), "SwinURNet: hybrid transformer-CNN architecture for real-time unstructured road segmentation," *IEEE. T. Instrum. Measur.*, **73**, 1-16, 5035816. https://doi.org/10.1109/TIM.2024.3470042.

Wu, Y., Kang, F., Zhang, Y., Li, X. and Li, H. (2024), "Structural identification of concrete dams with ambient vibration based on surrogate-assisted multi-objective salp swarm algorithm", *Structures*, **60**, 105956. https://doi.org/10.1016/j.istruc.2024.105956

Xiao, Z.Y., Li, Y.J., Zhang, W., Han, Y.J., Li, D., Chen, Q., Zeng, Z.M., Quan, Z.Y. and Xu, X.H. (2022), "Enhancement of torque efficiency and spin Hall angle driven collaboratively by orbital torque and spin-orbit torque", *Appl. Phys. Lett.*, **121**(7), 072404. https://doi.org/10.1063/5.0086125

Xie, J., Wen, M., Ding, P., Tu, Y., Wu, D., Liu, K., Tang, K. and Chen, M. (2024), "Interfacial flow contact resistance effect for thermal consolidation of layered viscoelastic saturated soils with semi-permeable boundaries", *Int. J. Num. Anal. Meth. Geomech.*, **48**(15), 3640-3679. https://doi.org/10.1002/nag.3805

Xin, J., Xu, W., Cao, B., Wang, T. and Zhang, S. (2024), "A deep-learning-based MAC for integrating channel access, rate adaptation and channel switch", *Comput. Sci., Netw. Internet. Arch.*, arXiv preprint arXiv:2406.02291. https://doi.org/10.48550/arXiv.2406.02291.

Xu, C., Zhu, M., Wang, Q., Cui, J., Huang, Y., Huang, X., ... and Zhang, X. (2023), "TROP2-directed nanobody-drug conjugate elicited potent antitumor effect in pancreatic cancer", *J. Nanobiotech.*, **21**, 410. https://doi.org/10.1186/s12951-023-02183-9

Yang, N., Zou, Y. and Arefi, M. (2023), "Bending results of graphene origami reinforced doubly curved shell", *Def. Tech.*, **35**, 198-210. https://doi.org/10.1016/j.dt.2023.11.017.

Yan, C., Feng, M., Wu, Z., Guo, Y., Dong, W., Wang, Y. and Mian, A. (2024), "Discriminative correspondence estimation for unsupervised RGB-D point cloud registration", *IEEE. T. Circ. Syst. Video. Tech.*, Early Access. https://doi.org/10.1109/TCSVT.2024.3480268.

Ye, W., Zang, Q., Liu, J., Yang, F. and Lin, G. (2023), "Three-dimensional bending and free vibration analyses of laminated cylindrical panel with/without elastic foundation using two-dimensional discrete method", *Soil. Dyn. Earthq. Eng.*, **168**, 107831. https://doi.org/10.1016/j.soildyn.2023.107831.

Yu, L., Lei, Y., Ma, Y., Liu, M., Zheng, J., Dan, D. and Gao, P. (2021) "A comprehensive review of fluorescence correlation spectroscopy", *Front. Phys.* **9**, 644450. https://doi.org/10.3389/fphy.2021.644450

Yu, Y., Fu, T., Wang, S. and Yang, C. (2025), "Dynamic response of novel sandwich structures with 3D sinusoid-parallel-hybrid honeycomb auxetic cores: The cores based on negative Poisson's ratio of elastic jump", *Eur. J. Mech. A Solids*, **109**, 105449. https://doi.org/10.1016/j.euromechsol.2024.105449.

Zhang, Y. and Zhuang, X. (2018a), "A softening-healing law for self-healing quasi-brittle materials: Analyzing with strong discontinuity embedded approach", *Eng. Fract. Mech.*, **192**, 290-306. https://doi.org/10.1016/j.engfracmech.2017.12.018

Zhang, Y. and Zhuang, X. (2018b), "Cracking elements: A self-propagating Strong Discontinuity embedded Approach for quasi-brittle fracture", *Finite. Elem. Anal. Des.*, **144**, 84-100. https://doi.org/10.1016/j.finel.2017.10.007

Zhang, Y. and Zhuang, X. (2019), "Cracking elements method for dynamic brittle fracture", *Theor. Appl. Fract. Mech.*, **102**, 1-9. https://doi.org/10.1016/j.tafmec.2018.09.015

Zhang, Y. and Mang, H.A. (2020), "Global cracking elements: A novel tool for Galerkin-based approaches simulating quasi-brittle fracture", *Int. J. Numer. Meth. Eng.*, **121**(11), 2462-2480. https://doi.org/10.1002/nme.6315

Zhang, Y. (2017), "Multi-slicing strategy for the three-dimensional discontinuity layout optimization (3D DLO)", *Int. J. Numer. Anal. Meth. Geomech.* **41**(4), 488-507. https://doi.org/10.1002/nag.2566

Zhang, Y., Zeiml, M., Pichler, C. and Lackner, R. (2014), "Model-based risk assessment of concrete spalling in tunnel linings under fire loading", *Eng. Struct.*, **77**, 207-215. https://doi.org/10.1016/j.engstruct.2014.02.033

Zhang, Y., Lackner, R., Zeiml, M. and Mang, H.A. (2015), "Strong discontinuity embedded approach with standard SOS formulation: Element formulation, energy-based crack-tracking strategy, and validations", *Comput. Meth. Appl. Mech. Eng.*, **287**, 335-366. https://doi.org/10.1016/j.cma.2015.02.001.

Zhang, Y., Zhuang, X. and Lackner, R. (2018), "Stability analysis of shotcrete supported crown of NATM tunnels with discontinuity layout optimization", *Int. J. Numer. Anal. Meth. Geomech.*, **42**(11), 1199-1216. https://doi.org/10.1002/nag.2775

Zhang, Y., Gao, Z., Li, Y. and Zhuang, X. (2020), "On the crack opening and energy dissipation in a continuum based disconnected crack model", *Finite. Elem. Anal. Des.*, **170**, 103333. https://doi.org/10.1016/j.finel.2019.103333

Zhang, Y., Yang, X., Wang, X. and Zhuang, X. (2021a), "A micropolar peridynamic model with non-uniform horizon for static damage of solids considering different nonlocal enhancements", *Theor. Appl. Fract. Mech.*, **113**, 102930. https://doi.org/10.1016/j.tafmec.2021.102930

Zhang, Y., Huang, J., Yuan, Y. and Mang, H.A. (2021b), "Cracking elements method with a dissipation-based arc-length approach", *Finite. Elem. Anal. Des.*, **195**, 103573. https://doi.org/10.1016/j.finel.2021.103573

Zhang, Y., Gao, Z., Wang, X. and Liu, Q. (2022a), "Predicting the pore-pressure and temperature of fire-loaded concrete by a hybrid neural network", *Int. J. Comput. Meth.*, **19**(8), 2142011. https://doi.org/10.1142/S0219876221420111

Zhang, Y., Wang, X., Wang, X. and Mang, H.A. (2022b), "Virtual displacement based discontinuity layout optimization", *Int. J. Numer. Meth. Eng.*, **123**(22), 5682-5694. https://doi.org/10.1002/nme.7084

Zhang, Y., Gao, Z., Wang, X. and Liu, Q. (2023a), "Image representations of numerical simulations for training neural networks", *Comput. Model. Eng. Sci.*, **134**(2), 821-833.

Zhang, M., Jiang, X. and Arefi, M. (2023b), "Dynamic formulation of a sandwich microshell considering modified couple stress and thickness-stretching", *Eur. Phys. J. Plus.* **138**, 227. https://doi.org/10.1140/epjp/s13360-023-03753-4

Zhang, K., Ye, Z., Qi, M., Cai, W., Saraiva, J.L., Wen, Y., Liu, G., Zhu, Z., Zhu, S. and Zhao, J. (2024a), "Water quality impact on fish behavior: A review from an aquaculture perspective", *Rev. Aquaculture*, **17**(1), e12985. https://doi.org/10.1111/raq.12985.

Zhang, X., Chen, H., Wang, Y., Gao, X., Wang, Z., Wang, N. and Zang, D. (2024b), "Ultrasound induced grain refinement of crystallization in evaporative saline droplets", *Ultrason. Sonochem.*, **107**, 106938, https://doi.org/10.1016/j.ultsonch.2024.106938.

Zhang, H.H., Chao, J.B., Wang, Y.W., Liu, Y., Yao, H.M., Zhao, Z.P. and Niu, K. (2024c), "5G base station antenna array with heatsink radome", *IEEE T. Antenn. Propag.*, **72**(3), 2270-2278 https://doi.org/10.1109/TAP.2024.3358378.

Zhang, T., Xu, S. and Zhang, W. (2024d), "New approach to feedback stabilization of linear discrete time-varying stochastic systems", *IEEE. T. Auto. Control*, Early Access. https://doi.org/10.1109/TAC.2024.3482119.

Zhao, S. Zhang, Y. Zhang, Y. Yang, J. Kitipornchai, S. (2021), "Graphene origami-enabled auxetic metallic metamaterials: An

atomistic insight", *Int. J. Mech. Sci.*, **212**, 106814. https://doi.org/10.1016/j.ijmecsci.2021.106814.

Zhao, Z., Zhang, H., Shiau, J., Du, W., Ke, L., Wu, F. and Bao, X. (2024), "Failure envelopes of rigid tripod pile foundation under combined vertical-horizontal-moment loadings in clay", *Appl. Ocean. Res.*, **150**, 104131. https://doi.org/10.1016/j.apor.2024.104131

Yu, X., Feng, B., Yao, M., Peng, J. and Yang, S. (2024), "Recent progress in modular electrochemical synthesis of hydrogen and high-value-added chemicals based on solid redox mediator", *Small*, 2310573. https://doi.org/10.1002/smll.202310573

Shi, X., Zhang, Y., Pujahari, A. and Mishra, S.K. (2025), "When latent features meet side information: A preference relation based graph neural network for collaborative filtering", *Exp. Syst. Appl.*, **260**, 125423. https://doi.org/10.1016/j.eswa.2024.125423

Xiao, Y., Yang, Y., Ye, D. and Zhang, J. (2024a), "Quantitative precision second-order temporal transformation based pose control for spacecraft proximity operations," *IEEE. T. Aeros. Elect. Syst.*, Early Access. https://doi.org/10.1109/TAES.2024.3469167.

Xiao, Y., Yang, Y., Ye, D. and Zhao, Y. (2024b), "Scaling-transformation based attitude tracking control for rigid spacecraft with prescribed time and prescribed bound", *IEEE. T. Aeros. Elect. Syst.*, Early Access. https://doi.org/10.1109/TAES.2024.3451454.

Xinde, L.I., Dunkin, F. and Dezert, J. (2024), "Multi-source information fusion: Progress and future", *Chinese J. Aeronaut.*, **37**(7), 24-58. https://doi.org/10.1016/j.cja.2023.12.009

Xue, W., Xu, C., Zhang, K., Cui, L., Huang, X., Nan, Y., Ju. D., Chang, X. and Zhang, X. (2024), "Enhancing antitumor efficacy of CLDN18.2-directed antibody-drug conjugates through autophagy inhibition in gastric cancer", *Cell Death Discov.*, **10**, 393. https://doi.org/10.1038/s41420-024-02167-0

Xu, C., Huang, X., Hu, Q., Xue, W., Zhou, K., Li, X., ... and Zhang, X. (2024a), "Modulating autophagy to boost the antitumor efficacy of TROP2-directed antibody-drug conjugate in pancreatic cancer", *Biomed. Pharmacotherapy.*, **180**, 117550. https://doi.org/10.1016/j.biopha.2024.117550

Xu, W., Aponte, E. and Vasanthakumar, P. (2024b), "The property (ωπ) (\omega{ \pi }) as a generalization of the a-Weyl theorem[J]", *AIMS Math.*, **9**(9), 25646-25658. https://doi.org/10.3934/math.20241253

CC